



# Responses in reef-building corals to wildfire emissions: Heterotrophic plasticity and calcification

Bo Qin<sup>a,c</sup>, Kefu Yu<sup>a,b,\*</sup>, Yichen Fu<sup>a</sup>, Yu Zhou<sup>a</sup>, Yanliu Wu<sup>a</sup>, Wenqian Zhang<sup>a</sup>, Xiaoyan Chen<sup>a,\*</sup>

<sup>a</sup> Guangxi Laboratory on the Study of Coral Reefs in the South China Sea, Coral Reef Research Center of China, School of Marine Sciences, Guangxi University, Nanning 530004, China

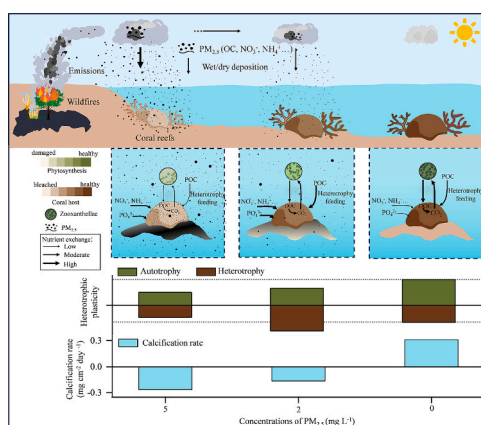
<sup>b</sup> Southern Marine Science and Engineering Guangdong Laboratory (Guangzhou), Guangzhou 511458, China

<sup>c</sup> School of Resources, Environment and Materials, Guangxi University, Nanning 530004, China

## HIGHLIGHTS

- Wildfire  $PM_{2.5}$  exposure impaired photosynthesis of *Porites lutea*.
- Coral symbionts adjusted nutrients strategies to adapt to wildfire stress.
- Enhanced heterotrophy sustained coral growth when autotrophy declined.
- Host heterotrophy was low under high levels of  $PM_{2.5}$ .
- Coral calcification was inhibited under both low and high levels of  $PM_{2.5}$ .

## GRAPHICAL ABSTRACT



## ARTICLE INFO

Editor: Olga Pantos

### Keywords:

Wildfire  $PM_{2.5}$   
Photoautotrophy  
Heterotrophic plasticity  
Stable isotopes  
Symbiodiniaceae  
Coral calcification

## ABSTRACT

Extreme wildfire events are on the rise globally, and although substantial wildfire emissions may find their way into the ocean, their impact on coral reefs remains uncertain. In a five-week laboratory experiment, we observed a significant reduction in photosynthesis in coral symbionts (*Porites lutea*) when exposed to fine particulate matter ( $PM_{2.5}$ ) from wildfires. At low  $PM_{2.5}$  level ( $2 mg L^{-1}$ ), the changes in  $\delta^{13}C$  and  $\delta^{15}N$  values in the host and symbiotic algae suggest reduced autotrophy and the utilization of wildfire particulates as a source of heterotrophic nutrients. This adaptive strategy, characterized by an increase in heterotrophy, sustained some aspects of coral growth (total biomass, proteins and lipids) under wildfire stress. Nevertheless, at high  $PM_{2.5}$  level ( $5 mg L^{-1}$ ), both autotrophy and heterotrophy significantly decreased, resulting in an imbalanced coral-algal nutritional relationship. These changes were related to light attenuation in seawater and particulate accumulation on the coral surface during  $PM_{2.5}$  deposition, ultimately rendering the coral growth unsustainable. Further, the calcification rates decreased by 1.5 to 1.85 times under both low and high levels of  $PM_{2.5}$ , primarily affected by

\* Corresponding authors at: Guangxi Laboratory on the Study of Coral Reefs in the South China Sea, Coral Reef Research Center of China, School of Marine Sciences, Guangxi University, Nanning 530004, China.

E-mail addresses: [kefuyu@scsio.ac.cn](mailto:kefuyu@scsio.ac.cn) (K. Yu), [xychen@gxu.edu.cn](mailto:xychen@gxu.edu.cn) (X. Chen).

<https://doi.org/10.1016/j.scitotenv.2024.171271>

Received 30 October 2023; Received in revised form 4 February 2024; Accepted 23 February 2024

Available online 28 February 2024

0048-9697/© 2024 Published by Elsevier B.V.

photosynthetic autotrophy rather than heterotrophy. Our study highlights a constrained heterotrophic plasticity of corals under wildfire stress. This limitation may restrict wildfire emissions as an alternative nutrient source to support coral growth and calcification, especially when oceanic food availability or autotrophy declines, as seen during bleaching induced by the warming ocean.

## 1. Introduction

The global increase in the frequency of wildfire events, attributed to climate warming (Jolly et al., 2015; Ruffault et al., 2020), is releasing substantial aerosols into the atmosphere. These wildfire aerosols primarily consist of fine particulate matter with a diameter <2.5  $\mu\text{m}$  (PM<sub>2.5</sub>), predominately composed of organic carbon (OC). PM<sub>2.5</sub> constitutes 80–90 % of smoke particulates generated from biomass burning (Fujii et al., 2014; Li et al., 2021b). These aerosols carry biogenic elements, e.g., soluble forms of nitrogen, phosphorus, and trace metals, especially iron (Barkley et al., 2019; Guieu et al., 2005; Schlosser et al., 2017). Emerging research suggests that wildfire aerosols can enter the ocean, potentially impacting marine biogeochemistry (Liu et al., 2022). Wildfire aerosols have the potential to trigger widespread phytoplankton blooms, impacting primary production (Abram et al., 2003; Ardyna et al., 2022; Tang et al., 2021). Certain toxic substances originating from wildfires, such as oxygenated polycyclic aromatic hydrocarbons (Xu et al., 2020a), have been found to adversely affect the resistance of sea otter to pathogen (Bowen et al., 2015). Coral reefs, recognized as the most biologically diverse marine ecosystem (Wall et al., 2020; Wiedenmann et al., 2013), are subject to the influence of wildfire emissions (Abram et al., 2003), although the specific impact remains unclear.

Some corals have the ability to ingest and digest organic components from sediment (Rosenfeld et al., 1999), including particulates smaller than 5  $\mu\text{m}$  (Kealoha et al., 2019). Recent studies have also identified some corals capable of ingesting microplastics (Reichert et al., 2022). This implies the potential for them to ingest wildfire PM<sub>2.5</sub>, which is rich in organic carbon and comprises non-living organic debris. The potential impact of wildfire PM<sub>2.5</sub> remains uncertain, and contrasting hypotheses are drawn from existing research on other suspended particulates and sediment sources, such as those from river runoffs and dredging activities. Previous investigations indicate terrestrial or detritus particles can have both beneficial and detrimental effects on corals. While they enhance coral lipid storage and tissue growth (Anthony, 2006), they could also harm corals by introducing suspended particulates, leading to diminished light intensity in the seawater and inhibiting photosynthetic capacity (Berry et al., 2016; Bessell-Browne et al., 2017b; Fisher et al., 2019; Jones et al., 2016). If unconsumed particulates attach to coral surfaces, they can increase mucus secretion, potentially causing energy depletion, reduced oxygen levels, and tissue damage (Bessell-Browne et al., 2017a; Jones et al., 2019). These factors ultimately reduce coral photosynthesis and feeding, leading to coral bleaching and mortality. The sublethal or lethal consequences could be further exacerbated when coupled with pollutants (Bejarano et al., 2022; Rogers, 1990). Moreover, corals might not always switch to a heterotrophic strategy when under stress. Some corals may deplete internal energy reserves (e.g., proteins, lipids, and carbohydrates) rather than actively capturing external food sources (Wall et al., 2019). The limited heterotrophic plasticity makes corals more susceptible to environmental stressors. Therefore, it is reasonable to hypothesize that wildfire PM<sub>2.5</sub> may have diverse impacts on corals. To understand the extent and underlying mechanisms of these impacts, further research is imperative.

Coral reefs primarily rely on nutrient exchange between corals host and its symbionts (Symbiodiniaceae) (Wall et al., 2020; Wiedenmann et al., 2013). This symbiotic relationship is essential for coral growth, calcification, and overall health (LaJeunesse et al., 2018; Price et al., 2021). However, environmental changes, such as ocean warming, acidification, shifting nutrients, sedimentation, and altered light

conditions can harm this partnership (Hoegh-Guldberg et al., 2007; Hughes et al., 2017), leading to Symbiodiniaceae loss, energy deficits, coral starvation, and higher mortality rates (Morris et al., 2019; Weis, 2008). It is worth noting that wildfires may intensify some of these changes, such as nutrient regimes or turbidity, through the oceanic deposition of wildfire emissions. For instance, forest fires in Sumatra and Kalimantan increase the levels of N and P in rainwater by 3–8 times compared to non-fire periods, and modeling suggests an increase of 86–100 % in seawater (Sundarambal et al., 2010). During the 2019 Australia wildfires, deposition fluxes of fire ash (including dust and black carbon) into adjacent seawaters exceeded 500 mg/m<sup>2</sup> (Tang et al., 2021). Some coral species adapt to these shifting conditions by displaying heterotrophic plasticity, adjusting between autotrophic and heterotrophic nutritional modes (Hughes et al., 2010; Wall et al., 2020). This transition involves relying on Symbiodiniaceae for photosynthesis during favorable conditions and capturing suspended zooplankton, phytoplankton and organic matter when conditions are less conducive (Houlbrèque and Ferrier-Pagès, 2009; Price et al., 2021). Heterotrophy meets 15 %–35 % of the daily metabolic demands in healthy corals and up to 100 % in bleached corals (Houlbrèque and Ferrier-Pagès, 2009; Price et al., 2021). Moreover, corals contribute to the formation of complex structural reef habitats for marine organisms through the processes of calcification. Recent studies in Kāneʻohe Bay showed that coral calcification rates correlate with their ingestion of small oceanic particulates (<5  $\mu\text{m}$ ) (Kealoha et al., 2019). When heterotrophic nutrients availability increases, corals allocate more energy to calcification, contributing up to 66 % of coral skeletal carbon (Houlbrèque and Ferrier-Pagès, 2009). The increased availability of light or energy together can increase the rates of coral calcification (Leuzinger et al., 2012). As ocean warming intensifies stratification and reduces marine productivity, corals may lose their common food sources from oceanic particulates, such as small zooplankton (Kealoha et al., 2019). In such circumstances, corals, especially in oligotrophic tropical and subtropical seas, may increasingly rely on atmospheric nutrient inputs in the absence of nutrients from both oceanic and land sources. However, it remains uncertain whether atmospheric deposition of wildfire emissions can act as alternative food sources for corals or induce environmental changes, such as reduced light intensity, nutrient enrichment, or sedimentation, with potential adverse effects on coral reefs.

In this research endeavor, we meticulously orchestrated a controlled laboratory experiment to scrutinize the nuanced impact of wildfire PM<sub>2.5</sub> on the intricate dynamics of the coral-algal relationship, heterotrophic feeding, energy reserves, and calcification mechanisms within *Porites lutea*. The investigation delved into the coral's responsiveness to two distinct concentrations of PM<sub>2.5</sub>, encompassing a comprehensive assessment of parameters such as photosynthesis efficiency, Symbiodiniaceae density, chlorophyll levels, tissue growth (including total biomass, proteins, and lipids), and calcification rates. Moreover, our analytical framework extended to the exploration of subtle shifts in the coral's nutritional adaptability. This was achieved by scrutinizing plasticity in  $\delta^{13}\text{C}$  and  $\delta^{15}\text{N}$  isotopic compositions in both the host coral and its symbiotic algae under varying PM<sub>2.5</sub> concentrations. This multifaceted approach aimed to unravel the intricate interplay between wildfire-induced emissions and the physiological intricacies of *P. lutea*, providing a comprehensive insight into the holistic effects on its ecological dynamics. These insights contribute significantly to the broader discourse on the ecological ramifications of wildfires on coral ecosystems, emphasizing the need for continued research and proactive conservation measures to safeguard these vulnerable marine organisms.

## 2. Materials and methods

### 2.1. Experimental design

Three experimental scenarios were designed as below:

- (1) The control treatment (C): No wildfire PM<sub>2.5</sub> input. Three coral samples were placed in a 5 L beaker. Water flow was simulated using a sinusoidal wave pump (SW-4: Jebao, China) (Fig. S1). Twenty percent of the seawater (1 L) was replaced daily for water exchange.
- (2) Low-concentration treatment (L-PM<sub>2.5</sub>): PM<sub>2.5</sub> input at 2 mg L<sup>-1</sup>, determined from mean values (3610 μg m<sup>-3</sup>) of the flux of PM<sub>2.5</sub> aerosols near a peatland fire (7120 μg m<sup>-3</sup>) (Fujii et al., 2014) and after long-distance transport (100 μg m<sup>-3</sup>) (Fujii et al., 2017). It was assumed that particulates enter a coral reef region at a depth of 3 m, uniformly mixing in seawater. Daily water changes included the introduction of PM<sub>2.5</sub> extracts. The wave pump simulated uniform mixing and resuspension of PM<sub>2.5</sub> and the removal of PM<sub>2.5</sub> on coral surfaces due to water flow. Other conditions were the same as those in the control treatment.
- (3) High-concentration treatment (H-PM<sub>2.5</sub>): PM<sub>2.5</sub> input at 5 mg L<sup>-1</sup>, determined based on a high flux of PM<sub>2.5</sub> aerosols near a peatland fire (7120 μg m<sup>-3</sup>) (Fujii et al., 2014). Other conditions were the same as those in the L-PM<sub>2.5</sub> treatment.

The coral samples (*P. lutea*) were collected by divers from Weizhou Island, China, with one coral divided into nine fragments (4 × 4 × 3 cm<sup>3</sup>), three fragments per treatment. All samples underwent a 15-day acclimatization period in a 216 L tank. Three beakers (one per treatment) were placed in the tank to ensure uniform light and temperature conditions. Seawater parameters were maintained at 26 ± 0.5 °C and a salinity of 33 ± 1 psu, with simulated natural light under a 12:12 light-dark cycle. The experiment lasted 35 days, with daily measurement of photosynthetic efficiency. Seawater nutrient levels were measured every three days. Assessment of coral color and PM<sub>2.5</sub> coverage on coral surfaces were conducted at 0, 14, 28, and 35 days. Buoyant weight for calcification was measured at 0 and 35 days, and other coral indices were assessed at the end of the experiment.

### 2.2. PM<sub>2.5</sub> collection

Wildfires PM<sub>2.5</sub> samples were collected by a high-volume sampler (Laoying 2031, Qingdao) within in a combustion simulation system (Fig. S2). Woody branches (1–8 cm diameter, 15–25 cm length) from subtropical trees (*Mangifera indica* L., *Litchi chinensis* Sonn., and *Dimocarpus longan* Lour.) were burned, and the resulting smoke was filtered onto quartz fiber membranes (GE Watman QMA, 203 × 254 mm) through a PM<sub>2.5</sub> impactor. Filters were heated at 450 °C for 5 h to remove organic carbon. The PM<sub>2.5</sub> content on filters was weighed using an analytical balance (SARTORIUS, BSA124S) with 0.1 mg accuracy.

PM<sub>2.5</sub> extracts were obtained by sonication of fiber membranes in 500 mL 0.45 μm-filtered seawater for 40 min (Li et al., 2021a). The recovery yield, determined by weighing PM<sub>2.5</sub> content in sonicated water against membrane content, was used to control the PM<sub>2.5</sub> input in the treatment. These extracts, mixed with seawater (1 L total), were added to treatment beaker daily.

### 2.3. Nutrient content and stable isotope analysis of PM<sub>2.5</sub> samples

Three randomly selected PM<sub>2.5</sub> samples were used for nutrient content and isotope analysis (Table 1). Nutrients leached from PM<sub>2.5</sub>, including the dissolved inorganic nitrogen (DIN = NO<sub>3</sub><sup>-</sup> + NO<sub>2</sub><sup>-</sup> + NH<sub>4</sub><sup>+</sup>) and soluble reactive phosphorus (SRP), were determined following the seawater analysis standard of China (GB 17378.4-2007). Ammonium was determined using the indophenol blue method. Nitrate was reduced

**Table 1**

Nutrient content and C and N isotope analysis of three independent PM<sub>2.5</sub> samples.

Parameters	PM <sub>2.5</sub> -1	PM <sub>2.5</sub> -2	PM <sub>2.5</sub> -3	Average value
NO <sub>3</sub> <sup>-</sup> + NO <sub>2</sub> <sup>-</sup> (μmol L <sup>-1</sup> )	2.2563	2.7233	3.1496	2.71 ± 0.45
NH <sub>4</sub> <sup>+</sup> (μmol L <sup>-1</sup> )	0.2370	0.4642	0.3690	0.36 ± 0.14
SRP (μmol L <sup>-1</sup> )	0.8654	0.6930	0.6759	0.74 ± 0.10
N/P	2.8810	4.5995	5.2057	4.22 ± 1.2
OC (%)	61.85	48.8221	39.9654	50.21 ± 11.00
δ <sup>15</sup> N <sub>Air</sub> ‰	21.43	11.17	17.80	16.8 ± 5.2
δ <sup>13</sup> C <sub>V-PDB</sub> ‰	-27.80	-28.10	-27.93	-27.94 ± 0.15

to nitrite by passing through a cadmium column, and its concentration was assessed using sulfanilamide/N-(1-naphthyl) ethylenediamine dihydrochloride method. The detected concentration includes nitrate and nitrite, expressed as NO<sub>3</sub><sup>-</sup> + NO<sub>2</sub><sup>-</sup>. Phosphate levels were measured through the phosphomolybdenum blue reaction. All nutrient analyses were conducted using an ultraviolet spectrophotometer (Shimadzu, UV-2700).

The fiber membranes containing PM<sub>2.5</sub> were acidified to remove carbonates before analyzing organic carbon (OC) and stable isotopes (Table 1). This process involved fumigating the membranes in open glass Petri dishes placed in a desiccator with concentrated HCl (12.1 mol L<sup>-1</sup>) for 24 h, followed by drying in an oven at 60 °C for 1 h (Kirillova et al., 2014). These treated membranes were then used to analyze OC content using an Elementar Vario EL Cube Elemental Analyzer. The remaining membranes were collected, sealed in a bag, and frozen for later isotope analysis of PM<sub>2.5</sub>, as described in Section 2.6.

### 2.4. Nutrient content in seawater

The concentrations of DIN and SRP in seawater from each beaker were measured using the method described in Section 2.3. For POC analysis, 1 L of seawater from each beaker was filtered under mild vacuum through pre-combusted Whatman GF/F filters (pore size 0.7 μm, 450 °C for 5 h), followed by freeze-drying for 24 h. POC content in seawater was determined using the same method (Luo et al., 2022) as described for the measurement of OC in PM<sub>2.5</sub> samples in Section 2.3.

### 2.5. Physiological analysis of corals

#### 2.5.1. Phenotypic parameters

Colorimetric change in corals was assessed for bleaching using images captured with the Olympus Tough TG-5 camera. Color squares ranging from white (D1, indicative of bleaching) to dark brown (D6, representing a healthy status) were matched to the D1–D6 color reference chart (Siebeck et al., 2006). Using ImageJ software, a correlation standard curve between D1–D6 levels and their grayscale values was established (Chow et al., 2016). Coral images were then converted to 8-bit grayscale, and the associated grayscale values for coral colors were analyzed and scored. Additionally, to estimate areal-coverage of PM<sub>2.5</sub> on coral surfaces, we outlined the PM<sub>2.5</sub> profile of each coral colony in ImageJ and calculated its planar area (Leinbach et al., 2021).

#### 2.5.2. Photochemical efficiency

The maximum dark-adapted photochemical efficiency (Fv/Fm) was measured using a pulse amplitude modulated fluorometer (PAM) (Monitoring-PAM, Walz, Germany) (Warner et al., 1999). Daily measurements were conducted after a 30-minute dark adaptation period, with the fiberoptic cable maintained approximately 1 mm from the coral surface, ensuring that Fo was adjusted within the recommended values (200–400 mV). Light intensity (photobiologically active radiation, PAR) inside the beaker was measured at 5-second intervals using a temperature/light recorder (Onset HOBO UA-002-08) equipped with a cosine light sensor.

### 2.5.3. Symbiodiniaceae density

Coral samples were placed on ice for subsequent treatments. Coral tissue was separated from the skeleton using a waterpik containing 0.45  $\mu\text{m}$ -filtered seawater. The initial volume of tissue slurry was measured using a graduated cylinder and then homogenized. Subsequently, 3 mL of coral homogenate was centrifuged (4000 r/min) for 5 min, and the resulting Symbiodiniaceae pellet was collected and preserved in 5 % formaldehyde (1 mL). Symbiodiniaceae densities were quantified microscopically using hemocytometer counts and normalized to the coral surface area. The normalization was based on correlations between the weight and surface area of aluminum foil imprints (Seemann, 2013; Xu et al., 2020b).

### 2.5.4. Chl-a content

Three 15 mL aliquots of coral homogenate were used to measure Chl-a content. After centrifugation (4000 r/min) for 5 min, the resulting precipitate was collected and stored at 4 °C. The pelleted algae were then resuspended in 100 % acetone for 24 h to rupture, followed by another recentrifuged (4000 r/min) for 5 min. Absorbance at wavelengths 750, 664, 647, and 630 nm were measured using a spectrophotometer (Shimadzu, UV-2700). Chl-a content was calculated using the equations provided by Jeffrey and Humphrey (1975).

### 2.5.5. Biomass, proteins and lipids in coral tissue

A 5 mL aliquot of coral homogenate was dried to a constant weight in a pre-combusted aluminum pan at 60 °C. Ashing was then performed at 500 °C for 4 h in a muffle furnace. The ash-free dry weight (total tissue biomass) was calculated by the difference between the dry and ash weights and standardized to surface area (Xu et al., 2021). To determine the total protein content, we employed the Shanghai Sangon BCA Protein Assay Kit and a Varioskan LUX Multimode Microplate Reader were used, following the method described in the literature (Smith et al., 1985). To assess total lipids in corals, a 0.5 mL aliquot of coral homogenate was lyophilized in a 10 mL tube. Freeze-drying was conducted for 48 h, followed by three rounds of ultrasonic extraction with a mixture of dichloromethane and methanol (2 mL: 2:1) for 10 min each. The resulting organic extracts were collected after centrifuging (500 g; 5 min), then freeze-dried and weighed to determine the total lipid content in  $\text{mg cm}^{-2}$  ( $\pm 0.01$  mg). The proportion of lipid content in the total tissue biomass was expressed in lipid percentage (Anthony et al., 2007; Teece et al., 2011).

### 2.5.6. Separation of symbiotic algae and host tissue

The remaining coral homogenates were centrifuged at 1500 rpm for 10 min. The resulting supernatant (host tissue) was filtered onto a pre-combusted Whatman GF/F filter with a 0.7  $\mu\text{m}$  pore size at 450 °C for 5 h. The filter was rinsed repeatedly with filtered seawater until Symbiodiniaceae were no longer detectable in the supernatant under a microscope. The collected Symbiodiniaceae pellet was resuspended three times in filtered seawater and purified twice by centrifugation. Both the filter membrane (host tissue) and Symbiodiniaceae pellets were washed in dilute HCl (1 mol  $\text{L}^{-1}$ ) to eliminate carbonates, followed by washing with distilled water and drying in an oven at 40 °C for 24 h (Alamaru et al., 2009; Seemann, 2013; Xu et al., 2020b). The resulting samples were collected, sealed in a bag, and frozen for later isotope analysis.

### 2.6. Net calcification rates

Net calcification rates were determined using the buoyant weighing technique (Vajed Samiei et al., 2016). Daily calcification rates were calculated by dividing the difference between initial and final weights by the number of days (n) and then standardized to the surface area. The formula used for this calculation is [(Final weight / Initial weight - 1) / n]  $\times$  100 % (Spencer Davies, 1989).

### 2.7. Stable isotope analysis

Stable isotope analysis involves assessing  $\delta^{13}\text{C}$  and  $\delta^{15}\text{N}$  in coral host ( $\delta^{13}\text{C}_h$ ,  $\delta^{15}\text{N}_h$ ), symbiont algae ( $\delta^{13}\text{C}_s$ ,  $\delta^{15}\text{N}_s$ ), and  $\text{PM}_{2.5}$  samples. The difference between the  $\delta^{13}\text{C}_h$  and  $\delta^{13}\text{C}_s$ , as well as  $\delta^{15}\text{N}_h$  and  $\delta^{15}\text{N}_s$ , is represented as  $\delta^{13}\text{C}_{h-s}$  and  $\delta^{15}\text{N}_{h-s}$ . These difference values are commonly used to assess the balance between heterotrophic and autotrophic nutrition and examine the nutritional relationship between coral host and symbiotic algae (Conti-Jerpe et al., 2020). The stable isotope analysis was conducted at the Third Institute of Oceanography, Ministry of Natural Resources, China. An elemental analyzer coupled with an isotope ratio mass spectrometer (CE Flash EA1112-Finnigan DeltaPlus XL) was used for these measurements. To ensure the precision and accuracy in the instrument's readings, a protein standard with a  $\delta^{13}\text{C}_{\text{V-PDB}}$  value of  $-26.98 \pm 0.13$  ‰ was introduced after every 10 samples. Each sample was replicated 2–3 times, and the final results were averaged.  $\delta^{13}\text{C}$  and  $\delta^{15}\text{N}$  values are reported relative to the Vienna Pee Dee Belemnite Limestone Standard (V-PDB). The long-term precision of the instrument is about  $\pm 0.2$  ‰ for C and  $\pm 0.25$  ‰ for N (Luo et al., 2022).

### 2.8. Statistical analysis

Statistical analysis was conducted using SPSS (Statistics 27, USA). All data are expressed as the mean  $\pm$  SD. One-way analysis of variance (ANOVA) was used to test significant differences between coral conditions under  $\text{PM}_{2.5}$  influence (Figs. 2c, 3b, 4, 5, 7a). Levene's test and Shapiro-Wilk's test were used to verify the assumptions of homoscedasticity and normality, and pairwise comparisons with post hoc Tukey's test were conducted to assess the level of significant differences. *t*-tests were also performed to examine the significant difference in Fv/Fm between the beginning and end of the experiment (Fig. 3b). Pearson's correlation was used to analyze the potential influence of Symbiodiniaceae density and  $\text{PM}_{2.5}$  coverage on coral growth, autotrophy and heterotrophy (Fig. 6a). It was also used to examine the influence of coral-algal nutrient relationship on coral growth (Fig. 6b). The coefficient of determination ( $R^2$ ) was derived from a regression model and used to explain the effects of autotrophy and heterotrophy on calcification (Fig. 7c-d). A *p*-value  $< 0.05$  was considered significant.

## 3. Results

### 3.1. Accumulated nutrients in seawater

In the control group, the average concentration of POC in seawater ranged from 0.27  $\text{mg L}^{-1}$  to 0.82  $\text{mg L}^{-1}$ . In the L- $\text{PM}_{2.5}$  group, it varied between 0.58  $\text{mg L}^{-1}$  to 2.00  $\text{mg L}^{-1}$ , showing a rapid increase on day 15 and consistently high values thereafter. In the H- $\text{PM}_{2.5}$  group, POC concentration fluctuated between 0.56  $\text{mg L}^{-1}$  and 3.54  $\text{mg L}^{-1}$ , following a similar trend to the L- $\text{PM}_{2.5}$  group after day 15 (Fig. 1b).

In the control group, the average concentrations of  $\text{NO}_3^-$  and  $\text{NO}_2^-$  in seawater ranged from  $1.69 \pm 0.04$   $\mu\text{mol L}^{-1}$  to  $3.75 \pm 0.26$   $\mu\text{mol L}^{-1}$  (Fig. 1c),  $\text{NH}_4^+$  ranged from  $0.50 \pm 0.01$   $\mu\text{mol L}^{-1}$  to  $1.02 \pm 0.04$   $\mu\text{mol L}^{-1}$  (Fig. 1d), and SRP from  $0.29 \pm 0.06$   $\mu\text{mol L}^{-1}$  to  $0.46 \pm 0.02$   $\mu\text{mol L}^{-1}$  (Fig. 1e).

In the L- $\text{PM}_{2.5}$  group, the average concentrations of  $\text{NO}_3^-$  and  $\text{NO}_2^-$  in seawater ranged from  $3.71 \pm 0.02$   $\mu\text{mol L}^{-1}$  to  $1.68 \pm 0.004$   $\mu\text{mol L}^{-1}$  (Fig. 1c),  $\text{NH}_4^+$  ranged from  $0.07 \pm 0.006$   $\mu\text{mol L}^{-1}$  to  $0.68 \pm 0.02$   $\mu\text{mol L}^{-1}$  (Fig. 1d), and SRP ranged from  $0.38 \pm 0.01$   $\mu\text{mol L}^{-1}$  to  $0.56 \pm 0.03$   $\mu\text{mol L}^{-1}$  (Fig. 1e). The DIN levels remained similar to those in the control group, while SRP increased and was higher than that in the control. The N/P ratio (3.4 to 10.15) indicated that the seawater was experiencing N limitation (Fig. 1f). The results show that low level wildfire  $\text{PM}_{2.5}$  may transport DIN that can be effectively absorbed, relieving N limitation for coral symbionts.

In the H- $\text{PM}_{2.5}$  group, the average concentration of  $\text{NO}_3^-$  and  $\text{NO}_2^-$  in seawater ranged from  $1.81 \pm 0.01$   $\mu\text{mol L}^{-1}$  to  $6.58 \pm 0.54$   $\mu\text{mol L}^{-1}$

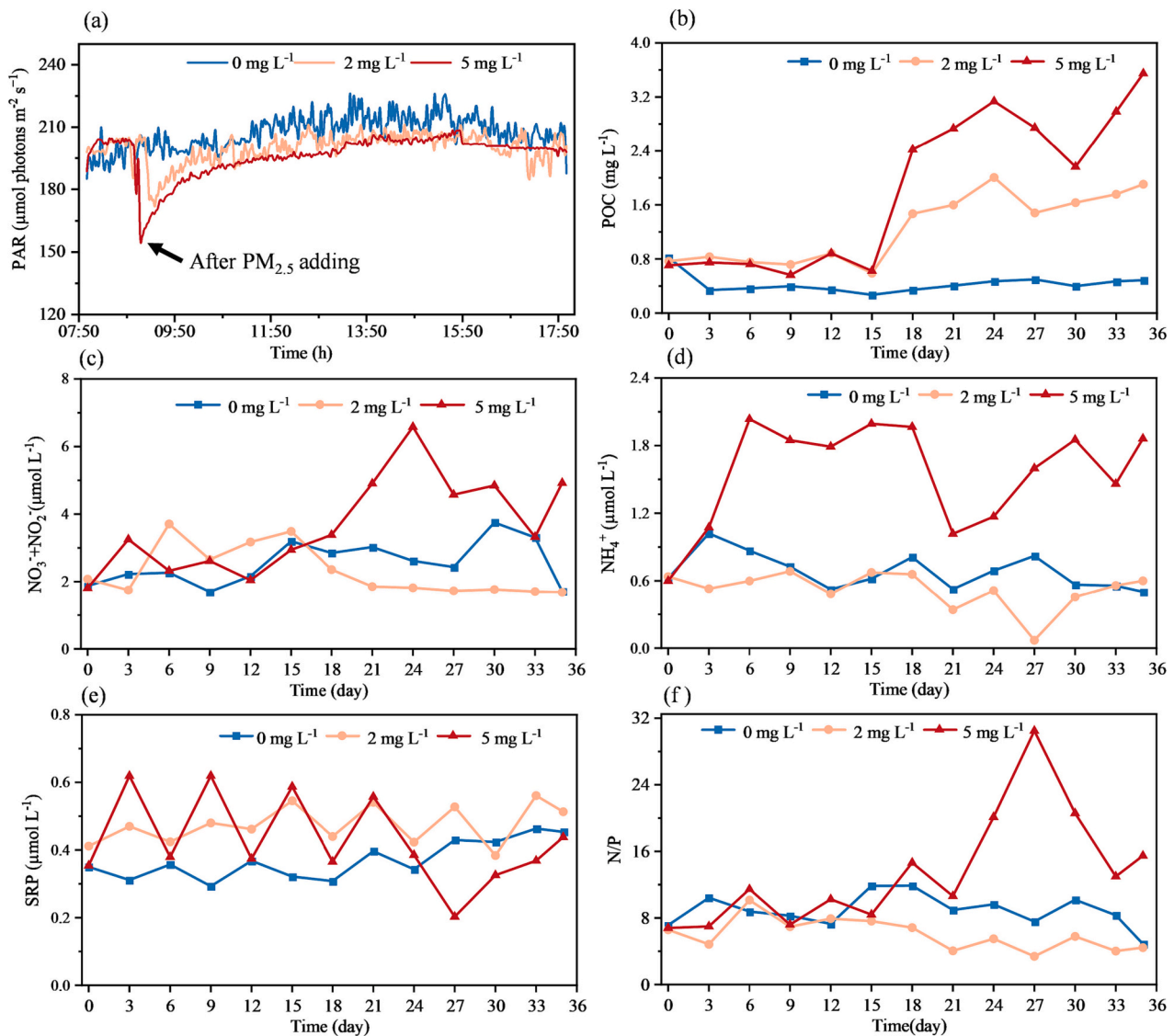


**Fig. 1.** Seawater environment in response to different  $PM_{2.5}$  deposition. (a) Photosynthetically Active Radiation; (b) Particulate Organic Carbon; (c) Nitrate and Nitrite; (d) Ammonium; (e) Soluble Reactive Phosphorus and (f) N/P Ratio. The PAR curve was recorded over a typical day at 5-second intervals, with a 50-point Savitzky-Golay smoothing.

(Fig. 1c),  $NH_4^+$  ranged from  $0.59 \pm 0.02 \mu mol L^{-1}$  to  $2.03 \pm 0.03 \mu mol L^{-1}$  (Fig. 1d), and SRP from  $0.20 \pm 0.09 \mu mol L^{-1}$  to  $0.62 \pm 0.01 \mu mol L^{-1}$  (Fig. 1e). The  $NO_3^-$  and  $NO_2^-$  initially resembled the control group but significantly increased after day 15, while  $NH_4^+$  started rising on day 6, suggesting that coral symbionts may have reached nitrogen saturation. SRP exhibited fluctuations throughout the experiment, with a sharp decrease on day 24, resulting in an imbalance nutrient supply ( $N/P = 12.96$  to  $20.5$ ), indicative of P limitation (Fig. 1f). The results suggest that high levels of wildfire  $PM_{2.5}$  could introduce excessive DIN, exceeding the absorption capacity of corals.

### 3.2. Coral phenotypic changes and bleaching

$PM_{2.5}$  exposure had visible effects on coral appearance and tentacle density (Fig. 2a). The control group remained healthy, displaying vibrant coloration (D6) and abundant tentacles (Fig. 2b and c). In contrast, the L- $PM_{2.5}$  group showed discoloration (D5) and minor particulates deposits (3–6 % coverage) between days 28–35, along with signs of tentacle retraction (Fig. 2b and c). The H- $PM_{2.5}$  group showed pronounced discoloration (D3), with  $PM_{2.5}$  covering  $20 \pm 0.01$  % of coral surfaces on day 14. This coverage increased to  $66 \pm 0.05$  % on day

28 and reached  $85 \pm 0.03$  % by day 35 (Fig. 2b and c).

### 3.3. Photosynthetic efficiency, Symbiodiniaceae density and pigment content

All three treatment groups exhibited declining Fv/Fm values in coral symbionts from day 1 to day 35 (Fig. 3a). The most significant decline occurred in the H- $PM_{2.5}$  group, falling from  $0.55 \pm 0.01$  to  $0.38 \pm 0.02$  (*t*-test,  $P < 0.05$ ; Fig. 3b, Table S2), below the healthy threshold of 0.5. The L- $PM_{2.5}$  group decreased from  $0.58 \pm 0.01$  to  $0.46 \pm 0.01$  (*t*-test,  $P < 0.05$ ; Fig. 3b, Table S2). The control group showed only a minor reduction, from  $0.56 \pm 0.01$  to  $0.53 \pm 0.02$  (*t*-test,  $P > 0.05$ ; Fig. 3b, Table S2). By the end of the experiment, Fv/Fm values were significantly lower in L- $PM_{2.5}$  and H- $PM_{2.5}$  groups compared to the control group (one-way ANOVA,  $F = 20.45$   $p < 0.05$ ; Table S4).

The density of Symbiodiniaceae decreased as the  $PM_{2.5}$  concentration increased, showing significant differences among all three groups (one-way ANOVA,  $F = 6.825$ ,  $p < 0.05$ ; Fig. 4a, Table S6). Specifically, the densities for the control, L- $PM_{2.5}$  and H- $PM_{2.5}$  groups were  $(2.72 \pm 0.48) \times 10^6$  cells  $cm^{-2}$ ,  $(1.75 \pm 0.40) \times 10^6$  cells  $cm^{-2}$ , and  $(0.83 \pm 0.04) \times 10^6$  cells  $cm^{-2}$ , respectively. There was no significant change in

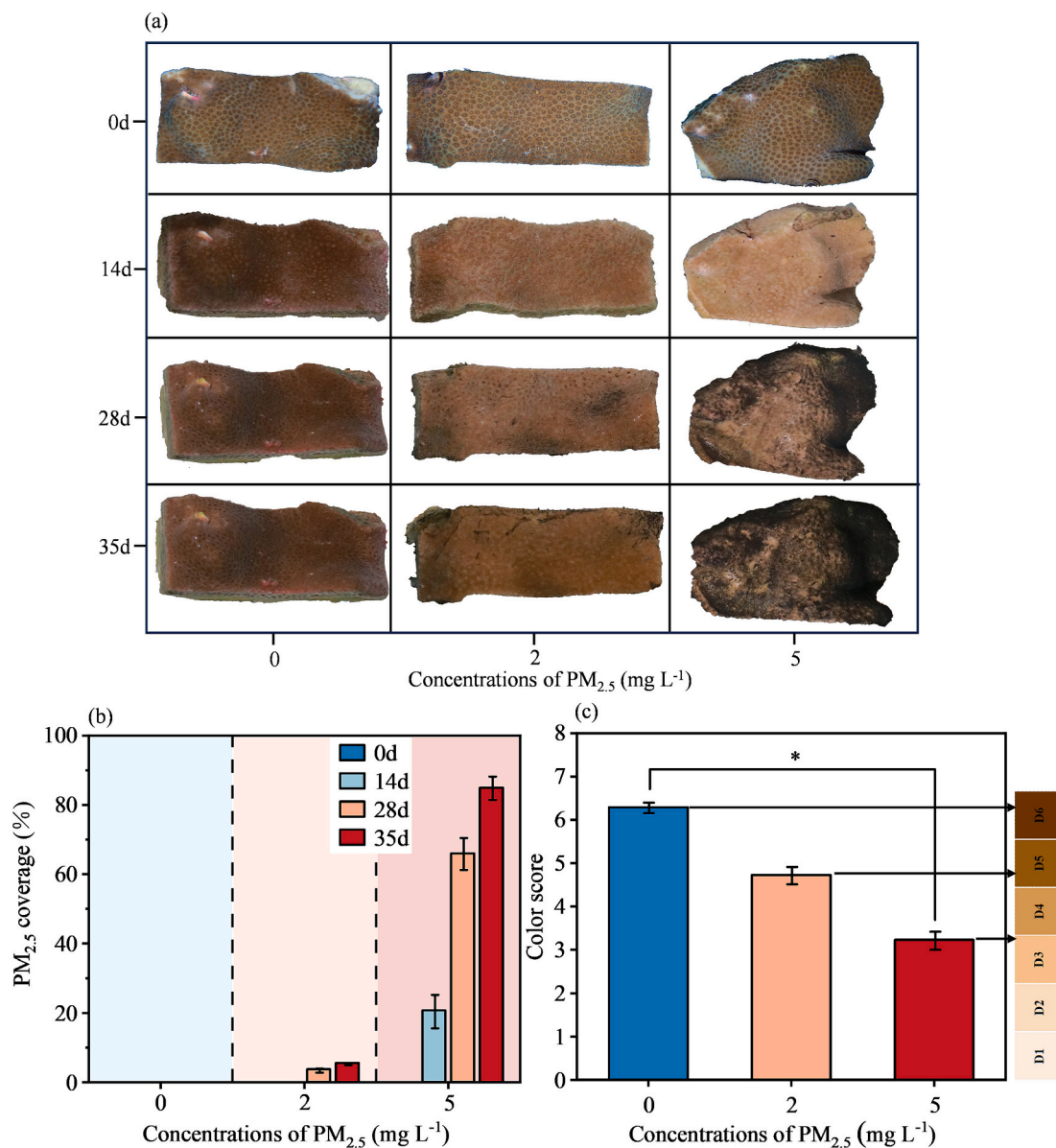


**Fig. 2.** Phenotypic changes in *P. lutea* under different PM<sub>2.5</sub> deposition. (a) Phototypic image; (b) PM<sub>2.5</sub> coverage on coral; (c) Bleaching pattern. The coral color was scored according to the D1–D6 color reference chart. \*,  $p < 0.05$ .

Symbiodiniaceae density in the L-PM<sub>2.5</sub> group compared to the control, while the H-PM<sub>2.5</sub> group had a significant lower density than the control.

The Chl-a content also decreased as the PM<sub>2.5</sub> concentration increased, showing significant differences among all three groups, with significantly lower values in the H-PM<sub>2.5</sub> groups compared to the control (one-way ANOVA,  $F = 10.546$ ,  $p < 0.05$ ; Fig. 4b, Table S6). The Chl-a contents for the control, L-PM<sub>2.5</sub> and H-PM<sub>2.5</sub> groups were  $16.62 \pm 1.55 \mu\text{g cm}^{-2}$ ,  $14.85 \pm 0.87 \mu\text{g cm}^{-2}$ , and  $9.43 \pm 0.91 \mu\text{g cm}^{-2}$ , respectively.

### 3.4. Total biomass, proteins and lipids contents

Coral samples exhibited higher levels of total biomass, proteins, and lipids in the L-PM<sub>2.5</sub> treatment compared to the control, while H-PM<sub>2.5</sub> treatment showed lower levels (Fig. 4c, d and e). Specifically: i) control group: biomass  $22.94 \pm 2.45 \text{ mg cm}^{-2}$ , proteins  $3.84 \pm 0.56 \text{ mg cm}^{-2}$ , lipids  $7.76 \pm 0.86 \text{ mg cm}^{-2}$ ; ii) L-PM<sub>2.5</sub> group: biomass  $26.51 \pm 1.81 \text{ mg cm}^{-2}$ , proteins  $5.28 \pm 0.36 \text{ mg cm}^{-2}$ , lipids  $8.62 \pm 0.75 \text{ mg cm}^{-2}$ ; iii) H-PM<sub>2.5</sub> group: biomass  $19.71 \pm 1.26 \text{ mg cm}^{-2}$ , proteins  $3.38 \pm 0.34 \text{ mg}$

$\text{cm}^{-2}$ , lipids  $6.44 \pm 0.37 \text{ mg cm}^{-2}$ . There were significant differences in proteins among all three groups, with significantly higher values in the L-PM<sub>2.5</sub> compared to the H-PM<sub>2.5</sub> groups (one-way ANOVA,  $F = 5.308$ ,  $p < 0.05$ ; Table S6). No statistically significance was observed for biomass (one-way ANOVA,  $F = 3.119$ ,  $p > 0.05$ ) and lipids (one-way ANOVA,  $F = 3.119$ ,  $p > 0.05$ ; Table S6).

The lipid percentages for the control, L-PM<sub>2.5</sub> and H-PM<sub>2.5</sub> groups were  $33.81 \pm 0.47 \%$ ,  $32.65 \pm 1.91 \%$ , and  $32.74 \pm 0.75 \%$ , respectively. Both lipid composition and proportion decreased in the PM<sub>2.5</sub> treatments, although there was no statistically significant difference (one-way ANOVA,  $F = 0.306$ ,  $p > 0.05$ ; Fig. 4f).

### 3.5. $\delta^{13}\text{C}$ and $\delta^{15}\text{N}$ values in coral host and symbiotic algae

The average values of  $\delta^{13}\text{C}_s$  value for the control, L-PM<sub>2.5</sub> and H-PM<sub>2.5</sub> group were  $-19.37 \pm 0.06 \%$ ,  $-19.63 \pm 0.17 \%$ , and  $-20.52 \pm 0.13 \%$ , respectively. There were no significant differences in  $\delta^{13}\text{C}_s$  values among all three groups (one-way ANOVA,  $F = 2.99$ ,  $p > 0.05$ ; Fig. 5a, Table S6). The average value of  $\delta^{13}\text{C}_h$  for the control, L-PM<sub>2.5</sub>

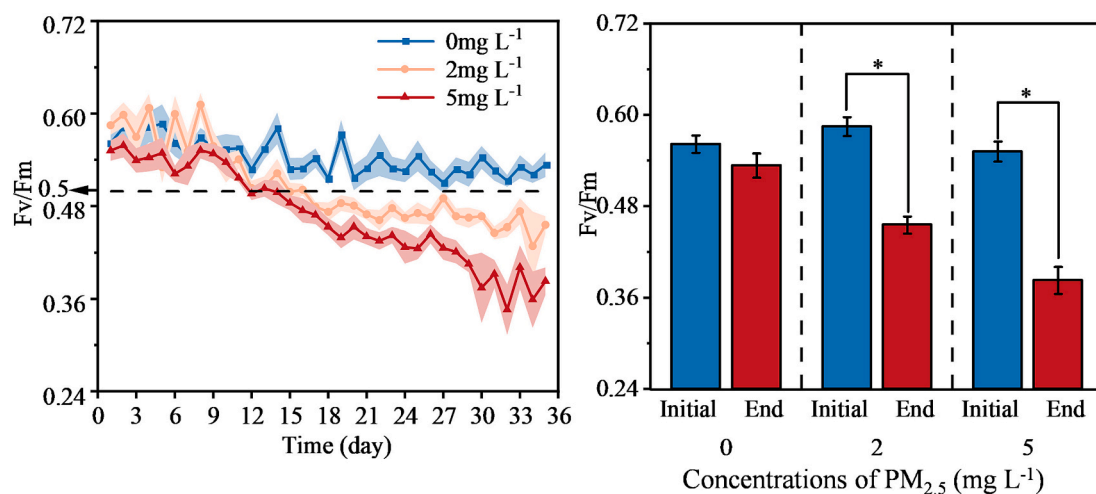


Fig. 3. Photosynthesis of *P. lutea* under different  $PM_{2.5}$  deposition. (a) Day-by-day photosynthetic efficiency; (b) Photochemical efficiency at the initial and end. \*,  $p < 0.05$ .

and H- $PM_{2.5}$  group was  $-18.17 \pm 0.01$  ‰,  $-18.39 \pm 0.22$  ‰, and  $-17.47 \pm 0.04$  ‰, respectively. Significant differences were found in the  $\delta^{13}C_h$  values among the groups, with significantly higher values in the H- $PM_{2.5}$  group than the other two groups (one-way ANOVA,  $F = 13.72$ ,  $p < 0.05$ ; Fig. 5a, Table S6). Additionally, the average values of  $\delta^{13}C_{h-s}$  were  $1.2 \pm 0.07$  ‰,  $1.24 \pm 0.037$  ‰, and  $3.1 \pm 0.15$  ‰, respectively. Statistically significant differences in  $\delta^{13}C_{h-s}$  were found among all the groups, with the H- $PM_{2.5}$  group differing significantly from the other two groups (one-way ANOVA,  $F = 9.27$ ,  $p < 0.05$ ; Fig. 5b, Table S6).

The average values of  $\delta^{15}N_s$  in the H- $PM_{2.5}$  group ( $9.35 \pm 0.08$  ‰) were significantly higher compared to both the control ( $8.27 \pm 0.03$  ‰) and L- $PM_{2.5}$  group ( $8.65 \pm 0.05$  ‰) (one-way ANOVA,  $F = 20.909$ ,  $p < 0.05$ ; Fig. 4c, Table S6). No significant differences in  $\delta^{15}N_h$  values were observed among the control ( $9.27 \pm 0.04$  ‰), L- $PM_{2.5}$  ( $9.61 \pm 0.15$  ‰) and H- $PM_{2.5}$  ( $9.30 \pm 0.04$  ‰) groups (one-way ANOVA,  $F = 3.56$ ,  $p > 0.05$ ; Fig. 4c, Table S6). The average values of  $\delta^{15}N_{h-s}$  showed significant differences among the groups (one-way ANOVA,  $F = 18.23$ ,  $p < 0.05$ ; Fig. 4d, Table S6). Specifically, the average values of  $\delta^{15}N_{h-s}$  in the H- $PM_{2.5}$  ( $-0.06 \pm 0.04$  ‰) were significantly lower than those in the control ( $1.00 \pm 0.06$  ‰) and L- $PM_{2.5}$  ( $0.96 \pm 0.11$  ‰) groups.

As showed in Fig. 5a, Symbiodiniaceae density positively correlated with  $\delta^{13}C_s$  and  $\delta^{15}N_{h-s}$  ( $r = 0.80$ ,  $0.73$ ,  $p < 0.05$ ), and negatively correlated with  $\delta^{15}N_s$  and  $\delta^{13}C_{h-s}$  ( $r = -0.79$ ,  $-0.73$ ,  $p < 0.05$ ).  $PM_{2.5}$  coverage positively correlated with  $\delta^{15}N_s$ ,  $\delta^{13}C_s$  and  $\delta^{13}C_{h-s}$  ( $r = 0.94$ ,  $0.87$ ,  $p < 0.05$ ), and negatively correlated with  $\delta^{13}C_s$  and  $\delta^{15}N_{h-s}$  ( $r = -0.79$ ,  $-0.73$ ,  $p < 0.05$ ). Additionally, except that  $\delta^{13}C_h$  negatively correlated with total biomass and lipid content ( $r = -0.77$ ,  $-0.74$ ,  $p < 0.05$ ), all other isotopic indicators (reflecting autotrophy or heterotrophy) did not exhibit significant correlation with the three coral growth parameters (Fig. 6b).

### 3.6. Net coral calcification rates

The net calcification rates significantly differed among all groups, being significantly lower in the H- $PM_{2.5}$  and L- $PM_{2.5}$  groups compared to the control group (one-way ANOVA,  $F = 107.69$ ,  $p < 0.001$ ; Fig. 7a, Table S6). The control group displayed an average net calcification rates of  $0.043 \pm 0.002$  %  $day^{-1}$ , indicating healthy coral growth. In contrast, the L- $PM_{2.5}$  group exhibited a calcification rate of  $-0.026 \pm 0.004$  %  $day^{-1}$ , and the H- $PM_{2.5}$  group had a rate of  $-0.05 \pm 0.007$  %  $day^{-1}$ .

No significant correlation observed between coral calcification rate and  $\delta^{13}C_h$  or  $\delta^{15}N_h$  (Fig. 7c and d). Instead, coral calcification rate positively correlated with zooxanthellae density and  $\delta^{13}C_s$  ( $R^2 = 0.57$ ,

$0.5$ ,  $p < 0.05$ ) (Fig. 7b and c), and negatively correlated with  $\delta^{15}N_s$  ( $R^2 = 0.63$ ,  $p < 0.05$ ) (Fig. 7d). The results indicated that coral calcification and autotrophy were primarily mediated by Symbiodiniaceae.

## 4. Discussions

### 4.1. Wildfire $PM_{2.5}$ impairs coral symbiont photosynthesis

The presence of wildfire  $PM_{2.5}$  in the surrounding seawater reduced light efficiency by 10–25 %, diminished the photochemical efficiency of coral symbionts, and led to a 40–70 % decrease in Symbiodiniaceae density (Figs. 1a, 3a and 4a). Under low light conditions, reduced photosynthesis efficiency can impede the growth and density of Symbiodiniaceae, as they struggled to access essential nutrients for photosynthesis (Jones et al., 2020; Wall et al., 2019). Exposure to sediment or suspended particulates from dredging activities (30–100  $mg L^{-1}$ ; 0.5–140  $\mu m$  in size) for 2–4 weeks can reduce Symbiodiniaceae density, pigment content and photosynthesis in corals, leading to visible coral bleaching (Bessell-Browne et al., 2017b; Jones et al., 2020). Moreover, the fine, dark carbonaceous particulates in wildfire  $PM_{2.5}$ , constituting ~50 % of the particulates, may have a more detrimental impact on photosynthesis. This is because that fine, darker-colored particulates (100–1000  $mg L^{-1}$ ;  $<63 \mu m$ ) more effectively reduce PAR compared to coarser, lighter-colored particulates (Storlazzi et al., 2015).

Disrupted photosynthesis may also be related to the deposition of wildfire  $PM_{2.5}$  on coral tissues. The extent of disruption varied with the duration and levels of  $PM_{2.5}$  exposure (Fig. 3a). During the initial 14 days, corals maintained a protective mucus layer. This mucus layer efficiently trapped tiny particulates and periodically shed them to keep the coral surface relatively clean (Bessell-Browne et al., 2017a; Precht, 2019). Benefiting from the protective role of mucus layer, the impact on photosynthesis in *M. peltiformis* corals is temporary when exposure to argillaceous sediment ( $<3 mm$ ), with subsequent recovery observed within 24–36 h (Bessell-Browne et al., 2017b; Philipp and Fabricius, 2003). However, by day 14, a large proportion (20.7–84.9 %) of coral surface was covered by  $PM_{2.5}$  (Fig. 2a and b). It appeared that the mucus failed to be removed; instead, it may combine with particulates to shade corals (Erfemeijer et al., 2012). Moreover, persistent stresses generally reduce coral mucus production (Bessell-Browne et al., 2017a), allowing  $PM_{2.5}$  to settle on coral surfaces and impede light acquisition. The results indicate that wildfire  $PM_{2.5}$  impaired coral clearance ability during extended exposure, especially at high levels. A similar phenomenon has been observed in prior study where sediment covering coral surfaces (66  $mg DW \cdot cm^{-2}$ ; +0.3 % and +0.6 % OC content;  $<63 \mu m$ ) induced

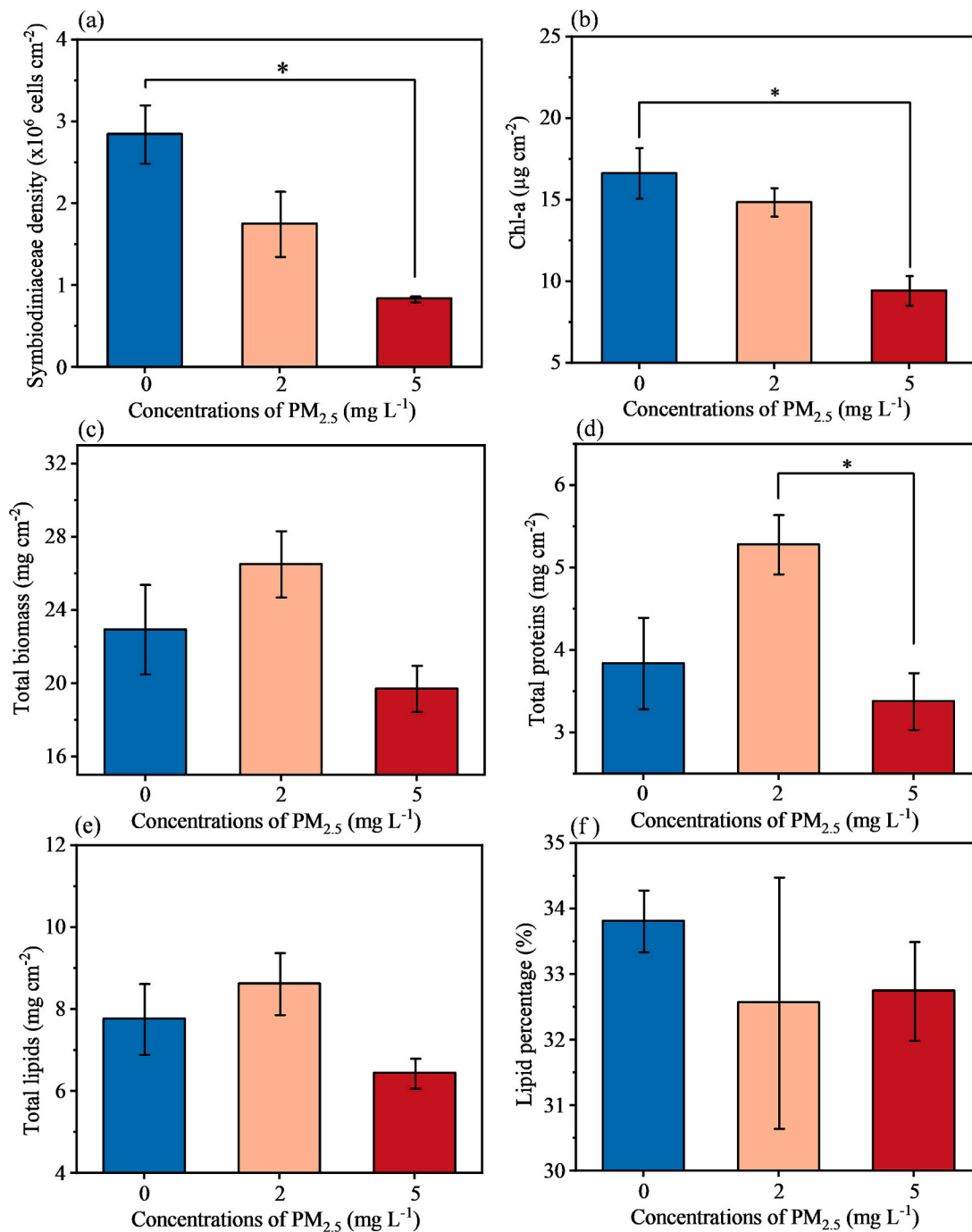


**Fig. 4.** Photosynthesis and growth of *P. lutea* under different PM<sub>2.5</sub> deposition. (a) Symbiodiniaceae density; (b) Chl-a content; (c) Total biomass; (d) Total protein content; (e) Total lipid content and (f) Lipid percentage. \*,  $p < 0.05$ .

hypoxia and a rapid decline in photosynthesis within 24 h (Weber et al., 2012). These findings suggest that while the corals survived the wildfire PM<sub>2.5</sub> stress, they experienced bleaching due to stresses such as diminished light and sedimentation, and the loss the density of symbiotic algae may compromise the coral-algal symbiotic relationship.

#### 4.2. Coral heterotrophic plasticity in response to wildfire PM<sub>2.5</sub>

##### 4.2.1. Nutrient strategies of symbiotic algae

The  $\delta^{13}\text{C}_s$  values decreased in the L-PM<sub>2.5</sub> treatment (by 0.26‰) and the H-PM<sub>2.5</sub> treatment (by 1.15‰) compared to the control, although the decreases were not statistically significant ( $p > 0.05$ ; Fig. 5a).  $\delta^{13}\text{C}_s$

values positively correlated with Symbiodiniaceae density ( $r = 0.80$ ,  $p < 0.05$ ; Fig. 6a). This correlation is because isotopic fractionation and  $\delta^{13}\text{C}$  values in symbiotic algae are primarily regulated by photosynthesis efficiency (Rodrigues and Grottole, 2006; Xu et al., 2020b; Xu et al., 2021). A higher Symbiodiniaceae density often boosts photosynthesis efficiency (Xu et al., 2020b). Increased photosynthesis and growth may induce carbon limitations, causing algae to reduce isotope discrimination (e.g., the preferential uptake of  $^{12}\text{C}$  during CO<sub>2</sub> assimilation) and increase  $\delta^{13}\text{C}_s$  values, and vice versa (Swart et al., 2005; Wall et al., 2019). Our results align with previous findings that  $\delta^{13}\text{C}_s$  values become more negative with decreasing light intensity associated with increasing water depth (Maier et al., 2010; Muscatine et al., 1989; Wall et al., 2020)

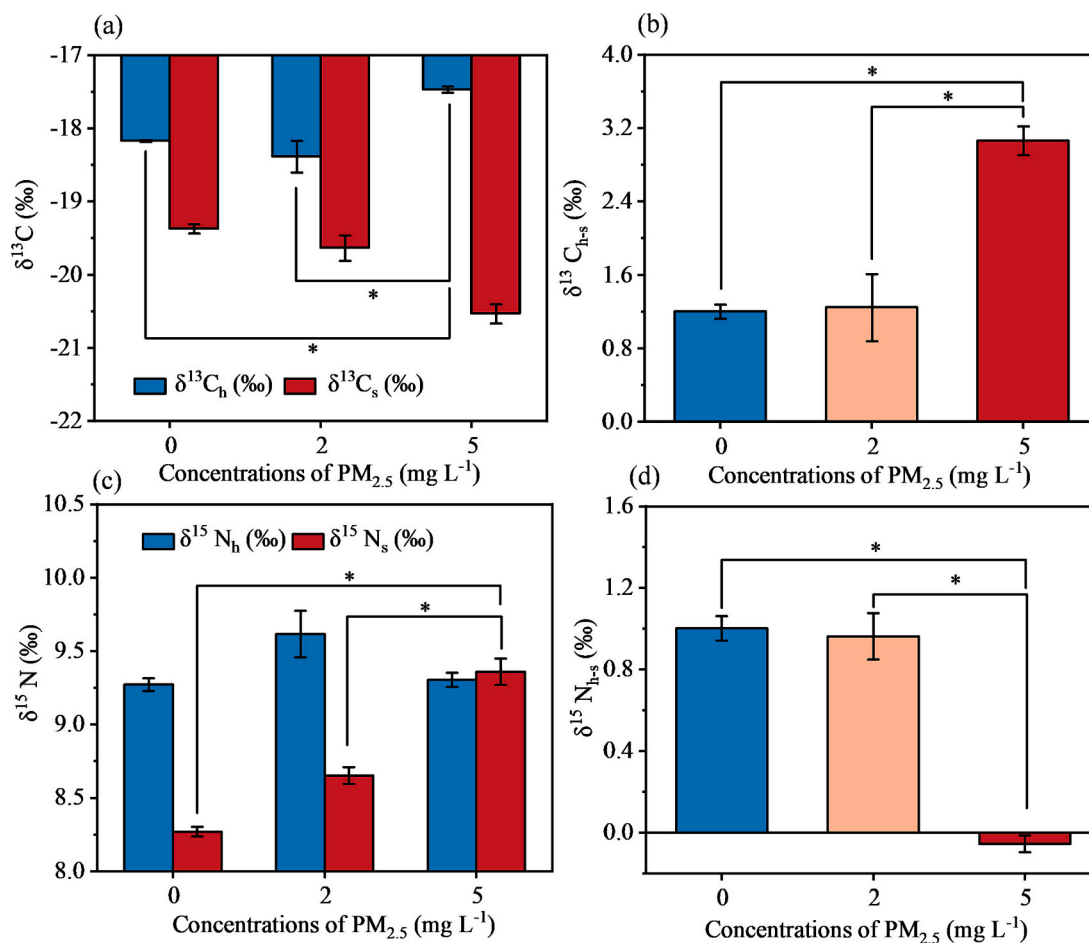


Fig. 5. Changes in  $\delta^{13}\text{C}$  and  $\delta^{15}\text{N}$  values of the coral host and symbiotic algae under different  $\text{PM}_{2.5}$  deposition. (a)  $\delta^{13}\text{C}_s$  and  $\delta^{13}\text{C}_h$ ; (b)  $\delta^{13}\text{C}_{h-s}$ ; (c)  $\delta^{15}\text{N}_h$  and  $\delta^{15}\text{N}_s$ ; (d)  $\delta^{15}\text{N}_{h-s}$ . The subscript “h” represents the isotopic values for the host, “s” for Symbiodiniaceae, and “h-s” for their differences. \*,  $p < 0.05$ .

or in turbid waters with reduced photosynthesis (Nahon et al., 2013), suggesting reduced autotrophy. Further, the greater  $\delta^{13}\text{C}_s$  declines in the H- $\text{PM}_{2.5}$  treatment may be related to coral bleaching (Fig. 2c). Due to the loss of symbiotic algae, bleached corals generally display lower  $\delta^{13}\text{C}_s$  values compared to corals during the recovery from bleaching stress (Wall et al., 2019). Corals with strong autotrophy can maintain a stable energy supply, enabling them to withstand environmental stressors (Xu et al., 2020b; Xu et al., 2021). The reduced autotrophy under wildfire stress implies a diminished energy supply to the host, compromising coral resistance to other environmental pressures.

The elevated  $\delta^{15}\text{N}_s$  values in the L- $\text{PM}_{2.5}$  (by 0.38 ‰;  $p > 0.05$ ) and the H- $\text{PM}_{2.5}$  (by 1.08 ‰;  $p < 0.05$ ) treatments compared to the control also suggested reduced autotrophy, especially under high wildfire stress (Fig. 5c).  $\delta^{15}\text{N}_s$  values negatively correlated with zooxanthellae density ( $r = -0.79$ ,  $p < 0.05$ ; Fig. 6a). During photosynthesis, there is usually a higher degree of isotopic fractionation, as symbiotic algae preferentially assimilate lighter nitrogen isotopes like  $^{14}\text{N}$  over  $^{15}\text{N}$  (Reynaud et al., 2009). The  $\delta^{15}\text{N}_s$  increase can be attributed to the loss of symbiotic algae (Fitt et al., 1993) and increased nitrogen uptake by the algae from seawater (Rodrigues and Grottoli, 2006), reducing nitrogen isotope fractionation (Schoepf et al., 2015). Symbiotic algae, experiencing reduced autotrophy, may prioritize seawater nutrients uptake for survival (Rodrigues and Grottoli, 2006). Wildfire  $\text{PM}_{2.5}$  carry biogenic elements, e.g., 2.48–3.15  $\mu\text{mol L}^{-1}$  DIN and other nutrients like SRP (Table 1). This process could lead to higher  $\delta^{15}\text{N}_s$  values, approaching those of wildfire  $\text{PM}_{2.5}$  (11.7 ‰–21.4 ‰; Table 1). Moreover, higher  $\delta^{15}\text{N}_s$  values are often observed during coral bleaching or recovery, because the loss of symbiotic algae relieves nitrogen limitation, allowing

the remaining algae to absorb more DIN to promote growth and recovery (Bessell-Browne et al., 2014; Rodrigues and Grottoli, 2006; Schoepf et al., 2015). This trend is evident during the initial stages after bleaching (Levas et al., 2013) and in the first month of recovery (Rodrigues and Grottoli, 2006). The timing of  $\delta^{15}\text{N}_s$  change aligns with our observations (35 days). Symbiotic algae may heterotrophically absorb wildfire nutrients (e.g., DIN) and translocate their products (e.g., amino acids) to the host, sustaining symbiont survival. However, the light attenuation due to wildfire particulates may hinder the effective promotion of photosynthesis and autotrophy by heterotrophic nutrients.

#### 4.2.2. Nutrient strategies of coral host

The  $\delta^{13}\text{C}_h$  values decreased by 0.22 ‰ in the L- $\text{PM}_{2.5}$  treatment compared to the control, although the difference is not statistically significant ( $p > 0.05$ ; Fig. 5a). This suggested a potential increase in host heterotrophy in response to  $\text{PM}_{2.5}$ , as the disrupted photosynthesis may have lowered nutrient supply for the host. Wildfire  $\text{PM}_{2.5}$  has lower  $\delta^{13}\text{C}$  values (−27.80 ‰ to −28.10 ‰) relative to corals (−13.4 ‰ to −21.6 ‰) (Fig. 5a, Table 1). As corals increase their reliance on heterotrophic feeding,  $\delta^{13}\text{C}_h$  values become more negative, approaching the  $\delta^{13}\text{C}$  range of their food sources like zooplankton and POC (−14 ‰ to −25 ‰) (Fox et al., 2019; Grottoli et al., 2017; Levas et al., 2013). For similar reasons, deeper-water corals typically display lower  $\delta^{13}\text{C}$  values due to reduced photosynthesis and increased consumption of isotopically depleted plankton compared to shallower corals (Alamaru et al., 2009; Fox et al., 2018; Muscatine et al., 1989). Similar patterns also hold in some productive areas when compared to oligotrophic waters (Levas et al., 2013; Rodrigues and Grottoli, 2006). Moreover, low  $\delta^{13}\text{C}_h$  can also

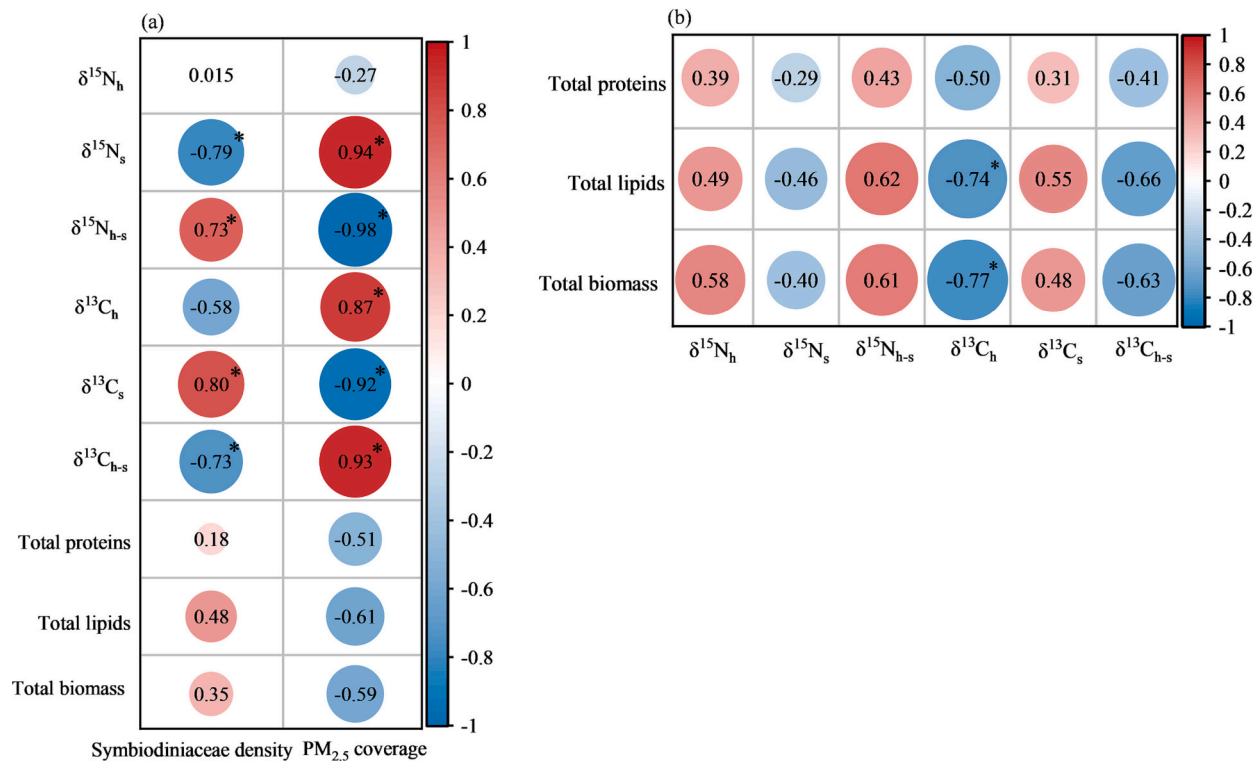


**Fig. 6.** Heatmap of the correlation between PM<sub>2.5</sub> deposition with parameters of coral growth and heterotrophic plasticity. The correlation coefficients between (a) heterotrophic plasticity (isotope values), coral growth (biomass, lipids and proteins) and photoautotrophy (Symbiodiniaceae)/PM<sub>2.5</sub> coverage; (b) coral growth and heterotrophic plasticity. \*,  $p < 0.05$ .

result from the preferential utilization of heterotrophic nutrition in lipid biosynthesis (Baumann et al., 2014; Wall et al., 2019). Reef corals exhibit lower  $\delta^{13}\text{C}$  values in lipids than in overall tissues (Hayes, 2001), and lipid breakdown may slightly increase  $\delta^{13}\text{C}$  values in the remaining organism (DeNiro and Epstein, 1977). In the L-PM<sub>2.5</sub> treatment, the lipid content increased, but the lipid proportion decreased (32.6 % vs. control 33.8 % vs. H-PM<sub>2.5</sub> 32.7 %) due to a larger increase in total biomass (Fig. 4f). Contrary to the anticipated increase in  $\delta^{13}\text{C}_h$  values due to the decrease in lipid proportion, the observed  $\delta^{13}\text{C}_h$  values were lower than those in the control and significantly lower than those in the H-PM<sub>2.5</sub> ( $p < 0.05$ ; Fig. 5a). The low observed  $\delta^{13}\text{C}_h$  values may be influenced by heterotrophic feeding on isotopically light wildfire PM<sub>2.5</sub>.

On the contrary, there was a significant increase in  $\delta^{13}\text{C}_h$  values (by 0.70 ‰) in the H-PM<sub>2.5</sub> treatment compared to the control ( $p < 0.05$ ) and significantly higher (by 0.92 ‰) compared to the L-PM<sub>2.5</sub> treatment ( $p < 0.05$ ), suggesting a reduction in heterotrophy (Fig. 5a). A positive correlation between  $\delta^{13}\text{C}_h$  and PM<sub>2.5</sub> coverage was observed (Fig. 5b,  $r = 0.87$ ,  $p < 0.05$ ). PM<sub>2.5</sub> coverage, as well as tentacle retraction and other particle-repelling actions, can impede the process of heterotrophic feeding on PM<sub>2.5</sub>. This perspective is corroborated by additional independent field studies on the effects of suspended particulates or sediment. For instance, corals displayed elevated  $\delta^{13}\text{C}_h$  and  $\delta^{13}\text{C}_{h-s}$  values in the productive coastal waters of Luhiutou in the northern SCS. This was due to the restriction of host heterotrophy in the severely turbid conditions of Luhiutou, as opposed to the oligotrophic, clear waters of the Xisha and Nansha Islands (Xu et al., 2021). With limited heterotrophy (due to zooplankton scarcity), corals (*Stylophora pistillata*) experienced elevated  $\delta^{13}\text{C}_h$  values during bleaching in the northern Red Sea and Gulf of Aqaba (Grottoli et al., 2017). Similarly, bleached corals initially exhibit higher  $\delta^{13}\text{C}_h$  values, which then significantly decrease after 1.5 months of recovery due to increased heterotrophic carbon uptake (Rodrigues and Grottoli, 2006). In the H-PM<sub>2.5</sub> treatment, both the lipid content and proportion decreased, although not statistically significant ( $p > 0.05$ ; Fig. 4e and f). The elevated  $\delta^{13}\text{C}_h$  values in the H-PM<sub>2.5</sub>

treatment were likely a result of corals catabolizing isotopically light lipids during bleaching (Grottoli and Rodrigues, 2011; Wall et al., 2019), rather than heterotrophic feeding on isotopically light wildfire PM<sub>2.5</sub>. These findings suggest that wildfire POC deposition has limited potential as an alternative heterotrophic source for corals.

The  $\delta^{15}\text{N}_h$  values increased by 0.34 ‰ in the L-PM<sub>2.5</sub> treatment compared to the control ( $p > 0.05$ ; Fig. 5c), suggesting a slight enhancement in heterotrophy. This may be attributed to the heterotrophic uptake of wildfire PM<sub>2.5</sub> containing DIN and OC (40–60 %) with higher  $\delta^{15}\text{N}$  values than corals (Table 1).  $\delta^{15}\text{N}_h$  values are often closely connected to the nitrogen sources originating from the base of the benthic food web (Dailer et al., 2010). In particle-rich waters, as coral heterotrophy increases,  $\delta^{15}\text{N}_h$  values rise, approaching the  $\delta^{15}\text{N}$  levels of the particles (Nahon et al., 2013). Seawater POC can significantly enrich  $\delta^{15}\text{N}_h$  values (Conti-Jerpe et al., 2020). In the Maldives, coral hosts, symbionts, and particulate organic matters at different depths displayed  $\delta^{15}\text{N}$  values aligned with upwelled deep-water nitrate sources (Radice et al., 2019). Thus, the  $\delta^{15}\text{N}_h$  values are influenced not only by symbiotic algae, with the  $\delta^{15}\text{N}$  values of DIN assimilated by symbionts ranging from 4 ‰ to 6 ‰ and that of N<sub>2</sub> fixed by diazotroph symbionts close to 0 ‰, but also by particulate detrital or living nitrogen sources (PON) taken by the host, which have higher  $\delta^{15}\text{N}$  (6 ‰–14 ‰) (Ferrier-Pagès and Leal, 2019). However, the lower values of  $\delta^{15}\text{N}_h$  in the H-PM<sub>2.5</sub> (by 0.31 ‰) compared to the L-PM<sub>2.5</sub> suggested a limitation of heterotrophic nitrogen uptake under high wildfire stress, potentially attributed to the same factors that limit heterotrophic carbon uptake, as discussed earlier for  $\delta^{15}\text{N}_h$ . However, the relatively minor changes in  $\delta^{15}\text{N}_h$  among the treatments did not show statistically significant differences, likely because of the relatively short duration of the experiment.

#### 4.2.3. Nutritional relationship between coral host and symbiotic algae

$\delta^{13}\text{C}_{h-s}$  and  $\delta^{15}\text{N}_{h-s}$  values are commonly used to assess the nutritional balance between coral hosts and symbiotic algae, gauging

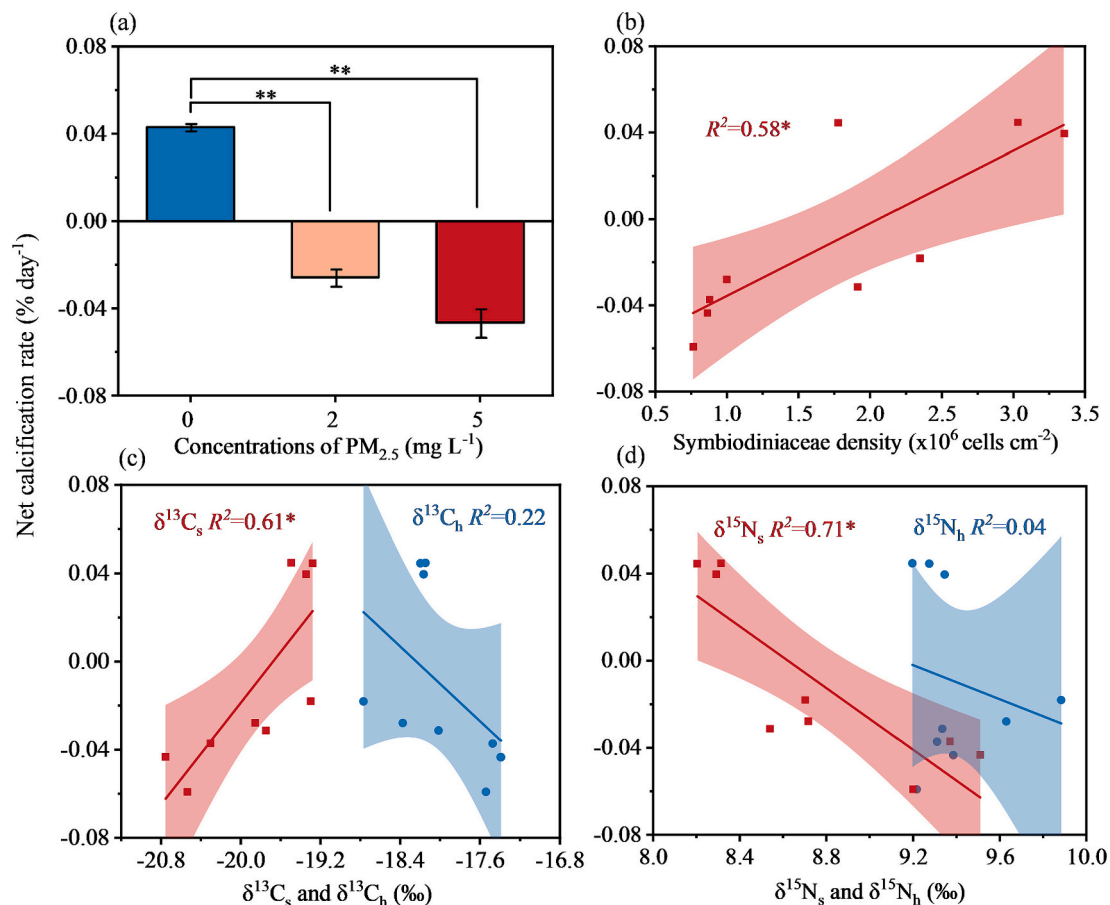


**Fig. 7.** Coral calcification under PM<sub>2.5</sub> deposition and its relationship with heterotrophic plasticity. (a) Net calcification rates of *P. lutea*. The relationship between calcification and (b) zooxanthellae density; (c) δ<sup>13</sup>C<sub>s</sub> or δ<sup>13</sup>C<sub>h</sub>; (d) δ<sup>15</sup>N<sub>h</sub> or δ<sup>15</sup>N<sub>s</sub>. \*,  $p < 0.05$ .

heterotrophic and autotrophic contributions (Conti-Jerpe et al., 2020). δ<sup>13</sup>C<sub>h-s</sub> values have strong inverse correlation with coral heterotrophy levels (Fox et al., 2019; Xu et al., 2020b), while δ<sup>15</sup>N<sub>h-s</sub> values tend to increase as photosynthetic efficiency decreases (Alamaru et al., 2009). In the L-PM<sub>2.5</sub> treatment, δ<sup>13</sup>C<sub>h-s</sub> and δ<sup>15</sup>N<sub>h-s</sub> values exhibited minor changes with higher standard errors compared to the control (Fig. 5b and d), suggesting a disturbance in the nutritional relationship but still maintaining relative balance. These differences, along with the decreases in δ<sup>13</sup>C<sub>h</sub> and δ<sup>13</sup>C<sub>s</sub> values and the increases in δ<sup>15</sup>N<sub>h</sub> and δ<sup>15</sup>N<sub>s</sub>, suggest a potential reduction in autotrophy and an enhancement of heterotrophy under low wildfire stress.

In the H-PM<sub>2.5</sub> treatment, there were increases in δ<sup>13</sup>C<sub>h</sub>, δ<sup>13</sup>C<sub>s</sub> and δ<sup>15</sup>N<sub>s</sub> values, while δ<sup>15</sup>N<sub>h</sub> values decreased, resulting in a significant increase in δ<sup>13</sup>C<sub>h-s</sub> compared to the control ( $p < 0.05$ ) and a shift of δ<sup>15</sup>N<sub>h-s</sub> from positive to negative values ( $p < 0.05$ ). These changes suggested reductions in both autotrophy and heterotrophy, with the latter being more pronounced, signifying a severe disruption and an imbalance in the nutrimental relationship. The presence of PM<sub>2.5</sub> coverage hampered heterotrophy, especially for carbon, impeding the uptake of POC. The host had to primarily rely on reduced autotrophy. Despite attempts by remaining symbiotic algae to absorb nutrients released by wildfire PM<sub>2.5</sub>, it proved insufficient to maintain the balance in the coral-algal relationship. Bleaching occurred, marked by a severe loss of symbiotic algae and a diminished photosynthesis rate (Fig. 3a-b). Abrupt increases in POC and nitrate levels coinciding with a rapid decline in Fv/Fm at Day 15 (Fig. 1b-d), along with consistently high NH<sub>4</sub><sup>+</sup> levels, indicated a disruption in metabolic processes (e.g., nitrogen assimilation) (Grover et al., 2003). Negative shifts in δ<sup>15</sup>N<sub>h-s</sub> values also suggest disruption of nitrogen cycling (Wang and Douglas, 1998) in bleached

corals and/or contributions of nitrogen not from host metabolism (Wall et al., 2019). Corals usually increase energy demand to resist environmental stresses, such as those associated with elevated temperature and sediment (Fisher et al., 2019). Therefore, the disruption of nutrient cycle may compromise coral tolerance to wildfire stress and other environmental changes.

When interpreting the isotopic differences, it is important to consider health status of corals (Price et al., 2021). In this study, the corals experienced bleaching under high wildfire stress, and the changes in δ<sup>13</sup>C<sub>h-s</sub> and δ<sup>15</sup>N<sub>h-s</sub> align with the patterns typically observed during coral bleaching. In bleached corals, like *S. pistillata*, δ<sup>13</sup>C<sub>h-s</sub> can significantly increase, indicating reduced heterotrophic carbon intake by the host (Grottoli et al., 2006, 2017; Swart et al., 2005; Wall et al., 2019). Bleaching can promptly induce significant changes in δ<sup>15</sup>N<sub>h-s</sub>, whereas non-bleached corals may experience only minor changes (Ferrier-Pagès et al., 2011; Radice et al., 2019; Reynaud et al., 2009). This difference can be attributed to the longer nitrogen turnover cycle in coral tissues, which spans 3 to 12 months, necessitating an extended period for noticeable variations in δ<sup>15</sup>N and δ<sup>15</sup>N<sub>h-s</sub> (Rangel et al., 2019; Tanaka et al., 2018). This may account for the minor changes in δ<sup>15</sup>N<sub>h</sub> and δ<sup>15</sup>N<sub>h-s</sub> under low wildfire stress, given the relatively shorter duration (35 days) and the limited signs of bleaching in the corals. Nevertheless, the imbalanced nutritional relationship between coral host and symbiotic algae suggested a limited heterotrophy plasticity under high wildfire stress.

### 4.3. Relationship between coral heterotrophy, growth and calcification

#### 4.3.1. Differential effects of wildfire $PM_{2.5}$ on coral energy reserves

Coral total biomass and lipids exhibited significant correlations with  $\delta^{13}C_h$  ( $r = -0.74, -0.77, p < 0.05$ ), while no significant relationships were observed with  $\delta^{13}C_z$  or  $\delta^{13}N_z$  (Fig. 5b). This suggested that coral growth under wildfire stress was primarily influenced by host heterotrophy rather than autotrophy. Coral growth was enhanced during the 35 days of exposure to low levels of  $PM_{2.5}$  (Fig. 3d, e and f). However, it is essential to note that this growth could be temporary, as observed in previous studies where *Montipora aequituberculata* corals displayed elevated protein and lipid levels after 4 weeks of exposure to 1 and 3 mg  $L^{-1}$  TSS. Over a 12-week period, these levels decreased due to particulate accumulation and sedimentation (Flores et al., 2012).

Under high wildfire stress, coral total proteins content were significantly reduced (Fig. 4d,  $p < 0.05$ ). There was also a decrease in total biomass and lipid content and the proportion of lipids in total biomass, although not significant (Fig. 4c, e, and f,  $p > 0.05$ ). The decreases could result from dual reductions in autotrophy and heterotrophy, potentially coupled with increased energy expenditure to resist wildfire stress. This involved managing water turbidity and particle-cleaning. Generally, coral tissue biomass and protein content decrease during bleaching due to reduced energy acquisition (Rodrigues and Grotto, 2006; Wall et al., 2019). Lipids, constituting 40–50 % of coral dry weight, serve as a crucial energy source during periods of energy insufficiency and photosynthesis deficits (Lesser, 2013). Water turbidity can reduce lipid production by Symbiodiniaceae and impede host heterotrophy, depleting lipid stores as energy acquisition declines (Anthony and Fabricius, 2000; Flores et al., 2012; Jones et al., 2020). The elevated  $\delta^{13}C_h$  values in the H- $PM_{2.5}$  treatment also suggested that coral likely catabolized isotopically light lipids, rather than heterotrophic feeding on isotopically light wildfire  $PM_{2.5}$ . On the other hand, corals usually increase their energy expenditure for defense processes (Bessell-Browne et al., 2017a; Flores et al., 2012). When exposed to sedimentation, corals utilize phagocytosis to eliminate foreign substances, leading to an increased respiratory rate (Flores et al., 2012). They also produce mucus to capture and expel particulates from the surroundings (Bessell-Browne et al., 2017a). The processes of particle clearance require the consumption of proteins, including antibodies and repair proteins (Wall et al., 2019). Coral biomass, lipids, energy content are critical for stress resilience and post-bleaching survival (Alamaru et al., 2009; Thornhill et al., 2011; Wall et al., 2019). Prior research has emphasized the importance of oceanic POC ( $<5 \mu m$ ) as an external nutrient source for corals (Kealoha et al., 2019). This study demonstrates that coral growth could be temporarily enhanced when wildfire  $PM_{2.5}$  promotes heterotrophy, however, as wildfire stress intensifies, the heterotrophy and coral growth may become unsustainable.

#### 4.3.2. Inhibited coral calcification under low/high levels of wildfire $PM_{2.5}$

It was surprising that corals experienced net dissolution under both low and high wildfire stresses, showing a decrease in net calcification rates ranging from 150 to 184 % (Fig. 6a). We observed a significant ( $p < 0.05$ ) coefficient of determination ( $R^2$ ) for Symbiodiniaceae density,  $\delta^{13}C_s$ ,  $\delta^{15}N_s$ , and calcification rates, ranging from 50 % to 63 % (Fig. 6b, c and d), suggesting the primary influence of autotrophy mediated by symbiotic algae on calcification. Coral calcification is closely linked to photosynthesis, as both processes rely on light (Suggett et al., 2013; Vajed Samiei et al., 2016). Calcification rates drop in low light, nearly threefold in complete darkness (Erftemeijer et al., 2012). Under high light conditions, *Acropora* sp. calcified 2.5 times faster ( $0.649 \text{ \% day}^{-1}$ ) compared to low light, and *S. pistillata* calcified 17 times faster ( $0.400 \text{ \% day}^{-1}$ ) (Reynaud-Vaganay et al., 2001). Reduced photosynthesis limits calcification by decreasing algal productivity. Bleaching typically reduces calcification, even if the remaining symbiotic algae photosynthesize more efficiently (Anthony et al., 2008). Reduced daytime photosynthesis lowers calcification, and bleached corals may reduce

calcification to conserve energy reserves or biomass, often accompanied by increased nighttime decalcification (Levas et al., 2013).

Further, reduced photosynthesis leads to decreased oxygen production, which is detrimental to calcification. Symbiont-produced oxygen promotes calcification, while oxygen deficiency limits host respiration and metabolic activities, including dark calcification (Holcomb et al., 2014). Additionally, the deposition of wildfire  $PM_{2.5}$  on coral surfaces can cause shading, further decreasing photosynthesis. Previous studies have demonstrated that sediment particulate coverage reduce photosynthesis, leading to hypoxia and increased energy expenditure for cleaning, protection, and repair, ultimately resulting in decreased calcification (Vajed Samiei et al., 2016). Calcification decreases when corals are exposed to coal particulates (2–4 weeks,  $38\text{--}275 \text{ mg L}^{-1}$ ,  $<63 \mu m$ ) (Berry et al., 2016), whether through long-term or acute contact with coal and sediments (Tretyakova et al., 2021). Moreover, high turbidity can physically damage coral reef structures through fragmentation and abrasion, further accelerating coral net dissolution efficiency (Erftemeijer et al., 2012). These findings collectively explain the observed decline in coral calcification due to wildfire  $PM_{2.5}$  in our experiment. While atmospheric POC is expected to supplement food availability from oceanic sources, thus offsetting the decline in coral calcification caused by ocean warming. However, this study suggests that wildfire particulates at moderate levels may enhance heterotrophy or other aspects of coral growth but may be insufficient to sustain calcification.

## 5. Conclusions

This laboratory study investigated the adaptive nutritional strategy of coral symbionts (*P. lutea*) in response to wildfire  $PM_{2.5}$  deposition, and its impact on coral growth and calcification. The findings revealed that autotrophy, the process by which corals produce their own food, decreased under wildfire stress. This reduction was linked to diminished Symbiodiniaceae density and decreased photosynthesis efficiency caused by light attenuation during  $PM_{2.5}$  deposition. At low levels of wildfire  $PM_{2.5}$ , autotrophy may decline, but the enhanced heterotrophic uptake of nutrients from wildfire  $PM_{2.5}$  could sustained coral growth. However, under high wildfire stress, both autotrophy and heterotrophy decreased, and the disruption could severely disturb the balance of nutrient exchange between the coral host and symbiotic algae, ultimately making coral growth unsustainable. The host's heterotrophic capacity largely depended on its ability to clear  $PM_{2.5}$  coverage on the coral surface, which was also associated with the duration and levels of  $PM_{2.5}$ . It is noteworthy that coral calcification declined under both low and high levels of wildfire  $PM_{2.5}$ , primarily influenced by photosynthesis and autotrophy. As oceanic POC tends to decrease in a warming ocean, corals may increasingly rely on atmospheric nutrients to support growth and calcification. However, this study suggests a constrained heterotrophy plasticity of corals under wildfire stress, which limits wildfire fine particulates as an alternative nutrient source to offset the declines in autotrophy.

### CRedit authorship contribution statement

**Bo Qin:** Data curation, Formal analysis, Methodology, Visualization, Writing – original draft. **Kefu Yu:** Funding acquisition, Project administration, Resources, Writing – review & editing. **Yichen Fu:** Investigation, Methodology. **Yu Zhou:** Formal analysis, Methodology, Software, Visualization. **Yanliu Wu:** Methodology, Software, Visualization. **Wenqian Zhang:** Methodology, Software, Visualization. **Xiaoyan Chen:** Conceptualization, Formal analysis, Funding acquisition, Methodology, Project administration, Writing – review & editing.

### Declaration of competing interest

The authors declare that they have no known competing financial

interests or personal relationships that could have appeared to influence the work reported in this paper.

## Data availability

Data will be made available on request.

## Acknowledgements

This work was funded by the National Science Foundation of China (42076157, 42090041 and 42030502). The authors wish to acknowledge Prof. Huiwang Gao for his constructive suggestions for the study on oceanic deposition of wildfire aerosols.

## Appendix A. Supplementary data

Supplementary data to this article can be found online at <https://doi.org/10.1016/j.scitotenv.2024.171271>.

## References

- Abram, N.J., Gagan, M.K., McCulloch, M.T., Chappell, J., Hantoro, W.S., 2003. Coral reef death during the 1997 Indian Ocean dipole linked to Indonesian wildfires. *Science* 301, 952–955. <https://doi.org/10.1126/science.1083841>.
- Alamaru, A., Loya, Y., Brokovich, E., Yam, R., Shemesh, A., 2009. Carbon and nitrogen utilization in two species of Red Sea corals along a depth gradient: insights from stable isotope analysis of total organic material and lipids. *Geochim. Cosmochim. Acta* 73, 5333–5342. <https://doi.org/10.1016/j.gca.2009.06.018>.
- Anthony, K., 2006. Enhanced energy status of corals on coastal, high-turbidity reefs. *Mar. Ecol. Prog. Ser.* 319, 111–116. <https://doi.org/10.3354/meps319111>.
- Anthony, K.R.N., Fabricius, K.E., 2000. Shifting roles of heterotrophy and autotrophy in coral energetics under varying turbidity. *J. Exp. Mar. Biol. Ecol.* 252, 221–253. [https://doi.org/10.1016/S0022-0981\(00\)00237-9](https://doi.org/10.1016/S0022-0981(00)00237-9).
- Anthony, K.R.N., Connolly, S.R., Hoegh-Guldberg, O., 2007. Bleaching, energetics, and coral mortality risk: effects of temperature, light, and sediment regime. *Limnol. Oceanogr.* 52, 716–726. <https://doi.org/10.4319/lo.2007.52.2.0716>.
- Anthony, K.R.N., Kline, D.L., Diaz-Pulido, G., Dove, S., Hoegh-Guldberg, O., 2008. Ocean acidification causes bleaching and productivity loss in coral reef builders. *Proc. Natl. Acad. Sci. USA* 105, 17442–17446. <https://doi.org/10.1073/pnas.0804478105>.
- Ardyna, M., Hamilton, D.S., Harmel, T., Lacour, L., Bernstein, D.N., Laliberté, J., Horvat, C., Laxenaire, R., Mills, M.M., Van Dijken, G., Polyakov, I., Claustre, H., Mahowald, N., Arrigo, K.R., 2022. Wildfire aerosol deposition likely amplified a summertime Arctic phytoplankton bloom. *Commun. Earth Environ.* 3, 201. <https://doi.org/10.1038/s43247-022-00511-9>.
- Barkley, A.E., Prospero, J.M., Mahowald, N., Hamilton, D.S., Popenдорf, K.J., Oehlert, A. M., Pournmand, A., Gatineau, A., Panichou-Pulcherie, K., Blackwell, P., Gaston, C. J., 2019. African biomass burning is a substantial source of phosphorus deposition to the Amazon, tropical Atlantic Ocean, and Southern Ocean. *Proc. Natl. Acad. Sci. USA* 116, 16216–16221. <https://doi.org/10.1073/pnas.1906091116>.
- Baumann, J., Grottoli, A.G., Hughes, A.D., Matsui, Y., 2014. Photoautotrophic and heterotrophic carbon in bleached and non-bleached coral lipid acquisition and storage. *J. Exp. Mar. Biol. Ecol.* 461, 469–478. <https://doi.org/10.1016/j.jembe.2014.09.017>.
- Bejarano, S., Diemel, V., Feuring, A., Ghilardi, M., Harder, T., 2022. No short-term effect of sinking microplastics on heterotrophy or sediment clearing in the tropical coral *Stylophora pistillata*. *Sci. Rep.* 12, 1468. <https://doi.org/10.1038/s41598-022-05420-7>.
- Berry, K.L.E., Hoogenboom, M.O., Flores, F., Negri, A.P., 2016. Simulated coal spill causes mortality and growth inhibition in tropical marine organisms. *Sci. Rep.* 6, 25894. <https://doi.org/10.1038/srep25894>.
- Bessell-Browne, P., Stat, M., Thomson, D., Clode, P.L., 2014. *Coscinaraea marshallae* corals that have survived prolonged bleaching exhibit signs of increased heterotrophic feeding. *Coral Reefs* 33, 795–804. <https://doi.org/10.1007/s00338-014-1156-z>.
- Bessell-Browne, P., Fisher, R., Duckworth, A., Jones, R., 2017a. Mucous sheet production in *Porites*: an effective bioindicator of sediment related pressures. *Ecol. Indic.* 77, 276–285. <https://doi.org/10.1016/j.ecolind.2017.02.023>.
- Bessell-Browne, P., Negri, A.P., Fisher, R., Clode, P.L., Duckworth, A., Jones, R., 2017b. Impacts of turbidity on corals: the relative importance of light limitation and suspended sediments. *Mar. Pollut. Bull.* 117, 161–170. <https://doi.org/10.1016/j.marpolbul.2017.01.050>.
- Bowen, L., Miles, A.K., Kolden, C.A., Saarinen, J.A., Bodkin, J.L., Murray, M.J., Tinker, M.T., 2015. Effects of wildfire on sea otter (*Enhydra lutris*) gene transcript profiles. *Mar. Mamm. Sci.* 31, 191–210. <https://doi.org/10.1111/mms.12151>.
- Chow, M.H., Tsang, R.H.L., Lam, E.K.Y., Ang, P., 2016. Quantifying the degree of coral bleaching using digital photographic technique. *J. Exp. Mar. Biol. Ecol.* 479, 60–68. <https://doi.org/10.1016/j.jembe.2016.03.003>.
- Conti-Jerpe, I.E., Thompson, P.D., Wong, C.W.M., Oliveira, N.L., Duprey, N.N., Moynihan, M.A., Baker, D.M., 2020. Trophic strategy and bleaching resistance in reef-building corals. *Sci. Adv.* 6, eaaz5443 <https://doi.org/10.1126/sciadv.aaz5443>.
- Dailer, M.L., Knox, R.S., Smith, J.E., Napier, M., Smith, C.M., 2010. Using  $\delta^{15}\text{N}$  values in algal tissue to map locations and potential sources of anthropogenic nutrient inputs on the island of Maui, Hawai'i, USA. *Mar. Pollut. Bull.* 60, 655–671. <https://doi.org/10.1016/j.marpolbul.2009.12.021>.
- DeNiro, M.J., Epstein, S., 1977. Mechanism of carbon isotope fractionation associated with lipid synthesis. *Science* 197, 261–263. <https://doi.org/10.1126/science.327543>.
- Erfteimeijer, P.L.A., Riegl, B., Hoeksema, B.W., Todd, P.A., 2012. Environmental impacts of dredging and other sediment disturbances on corals: a review. *Mar. Pollut. Bull.* 64, 1737–1765. <https://doi.org/10.1016/j.marpolbul.2012.05.008>.
- Ferrier-Pagès, C., Leal, M.C., 2019. Stable isotopes as tracers of trophic interactions in marine mutualistic symbioses. *Ecol. Evol.* 9, 723–740. <https://doi.org/10.1002/ece3.4712>.
- Ferrier-Pagès, C., Peirano, A., Abbate, M., Cocito, S., Negri, A., Rottier, C., Riera, P., Rodolfo-Metalpa, R., Reynaud, S., 2011. Summer autotrophy and winter heterotrophy in the temperate symbiotic coral *Cladocora caespitosa*. *Limnol. Oceanogr.* 56, 1429–1438. <https://doi.org/10.4319/lo.2011.56.4.1429>.
- Fisher, R., Bessell-Browne, P., Jones, R., 2019. Synergistic and antagonistic impacts of suspended sediments and thermal stress on corals. *Nat. Commun.* 10, 2346. <https://doi.org/10.1038/s41467-019-10288-9>.
- Fitt, W.K., Spero, H.J., Halas, J., White, M.W., Porter, J.W., 1993. Recovery of the coral *Montastrea annularis* in the Florida Keys after the 1987 Caribbean “bleaching event”. *Coral Reefs* 12, 57–64. <https://doi.org/10.1007/BF00302102>.
- Flores, F., Hoogenboom, M.O., Smith, L.D., Cooper, T.F., Abrego, D., Negri, A.P., 2012. Chronic exposure of corals to fine sediments: lethal and sub-lethal impacts. *PLoS One* 7, e37795. <https://doi.org/10.1371/journal.pone.0037795>.
- Fox, M.D., Williams, G.J., Johnson, M.D., Radice, V.Z., Zgliczynski, B.J., Kelly, E.L.A., Rohwer, F.L., Sandin, S.A., Smith, J.E., 2018. Gradients in primary production predict trophic strategies of mixotrophic corals across spatial scales. *Curr. Biol.* 28, 3355–3363.e4. <https://doi.org/10.1016/j.cub.2018.08.057>.
- Fox, M.D., Elliott Smith, E.A., Smith, J.E., Newsome, S.D., 2019. Trophic plasticity in a common reef-building coral: insights from  $\delta^{13}\text{C}$  analysis of essential amino acids. *Funct. Ecol.* 33, 2203–2214. <https://doi.org/10.1111/1365-2435.13441>.
- Fujii, Y., Iriana, W., Oda, M., Puriwigati, A., Tohno, S., Lestari, P., Mizohata, A., Huboyo, H.S., 2014. Characteristics of carbonaceous aerosols emitted from peatland fire in Riau, Sumatra, Indonesia. *Atmos. Environ.* 87, 164–169. <https://doi.org/10.1016/j.atmosenv.2014.01.037>.
- Fujii, Y., Tohno, S., Amil, N., Latif, M.T., 2017. Quantitative assessment of source contributions to PM<sub>2.5</sub> on the west coast of Peninsular Malaysia to determine the burden of Indonesian peatland fire. *Atmos. Environ.* 171, 111–117. <https://doi.org/10.1016/j.atmosenv.2017.10.009>.
- Grottoli, A.G., Rodrigues, L.J., 2011. Bleached *Porites compressa* and *Montipora capitata* corals catabolize  $\delta^{13}\text{C}$ -enriched lipids. *Coral Reefs* 30, 687. <https://doi.org/10.1007/s00338-011-0756-0>.
- Grottoli, A.G., Rodrigues, L.J., Palardy, J.E., 2006. Heterotrophic plasticity and resilience in bleached corals. *Nature* 440, 1186–1189. <https://doi.org/10.1038/nature04565>.
- Grottoli, A.G., Tchernov, D., Winters, G., 2017. Physiological and biogeochemical responses of super-corals to thermal stress from the northern Gulf of Aqaba, Red Sea. *Front. Mar. Sci.* 4, 215. <https://doi.org/10.3389/fmars.2017.00215>.
- Grover, R., Maguer, J.-F., Allemand, D., Ferrier-Pagès, C., 2003. Nitrate uptake in the scleractinian coral *Stylophora pistillata*. *Limnol. Oceanogr.* 48, 2266–2274. <https://doi.org/10.4319/lo.2003.48.6.2266>.
- Guieu, C., Bonnet, S., Wagener, T., Loÿe-Pilot, M.-D., 2005. Biomass burning as a source of dissolved iron to the open ocean? *Geophys. Res. Lett.* 32, L19608. <https://doi.org/10.1029/2005GL022962>.
- Hayes, J.M., 2001. Fractionation of carbon and hydrogen isotopes in biosynthetic processes. *Rev. Mineral. Geochem.* 43, 225–277. <https://doi.org/10.2138/gsrmg.43.1.225>.
- Hoegh-Guldberg, O., Mumby, P.J., Hooten, A.J., Steneck, R.S., Greenfield, P., Gomez, E., Harvell, C.D., Sale, P.F., Edwards, A.J., Caldeira, K., Knowlton, N., Eakin, C.M., Iglesias-Prieto, R., Muthiga, N., Bradbury, R.H., Dubi, A., Hatziozols, M.E., 2007. Coral reefs under rapid climate change and ocean acidification. *Science* 318, 1737–1742. <https://doi.org/10.1126/science.1152509>.
- Holcomb, M., Tambutté, E., Allemand, D., Tambutté, S., 2014. Light enhanced calcification in *Stylophora pistillata*: effects of glucose, glycerol and oxygen. *PeerJ* 2, e375. <https://doi.org/10.7717/peerj.375>.
- Houlbrèque, F., Ferrier-Pagès, C., 2009. Heterotrophy in tropical scleractinian corals. *Biol. Rev.* 84, 1–17. <https://doi.org/10.1111/j.1469-185X.2008.00058.x>.
- Hughes, A., Grottoli, A., Pease, T., Matsui, Y., 2010. Acquisition and assimilation of carbon in non-bleached and bleached corals. *Mar. Ecol. Prog. Ser.* 420, 91–101. <https://doi.org/10.3354/meps08866>.
- Hughes, T.P., Barnes, M.L., Bellwood, D.R., Cinner, J.E., Cumming, G.S., Jackson, J.B.C., Kleypas, J., Van De Leemput, I.A., Lough, J.M., Morrison, T.H., Palumbi, S.R., Van Nes, E.H., Scheffer, M., 2017. Coral reefs in the Anthropocene. *Nature* 546, 82–90. <https://doi.org/10.1038/nature22901>.
- Jeffrey, S.W., Humphrey, G.F., 1975. New spectrophotometric equations for determining chlorophylls a, b, c1 and c2 in higher plants, algae and natural phytoplankton. *Biochem. Physiol. Pflanz.* 167, 191–194. [https://doi.org/10.1016/S0015-3796\(17\)30778-3](https://doi.org/10.1016/S0015-3796(17)30778-3).
- Jolly, W.M., Cochrane, M.A., Freeborn, P.H., Holden, Z.A., Brown, T.J., Williamson, G.J., Bowman, D.M.J.S., 2015. Climate-induced variations in global wildfire danger from 1979 to 2013. *Nat. Commun.* 6, 7537. <https://doi.org/10.1038/ncomms8537>.
- Jones, R., Bessell-Browne, P., Fisher, R., Klonowski, W., Slivkoff, M., 2016. Assessing the impacts of sediments from dredging on corals. *Mar. Pollut. Bull.* 102, 9–29. <https://doi.org/10.1016/j.marpolbul.2015.10.049>.

- Jones, R., Fisher, R., Bessell-Browne, P., 2019. Sediment deposition and coral smothering. *PLoS One* 14, e0216248. <https://doi.org/10.1371/journal.pone.0216248>.
- Jones, R., Giofre, N., Luter, H.M., Neoh, T.L., Fisher, R., Duckworth, A., 2020. Responses of corals to chronic turbidity. *Sci. Rep.* 10, 4762. <https://doi.org/10.1038/s41598-020-61712-w>.
- Kealoha, A.K., Shamberger, K.E.F., Reid, E.C., Davis, K.A., Lentz, S.J., Brainard, R.E., Oliver, T.A., Rappé, M.S., Roark, E.B., Rii, Y.M., 2019. Heterotrophy of oceanic particulate organic matter elevates net ecosystem calcification. *Geophys. Res. Lett.* 46, 9851–9860. <https://doi.org/10.1029/2019GL083726>.
- Kirilova, E.N., Andersson, A., Han, J., Lee, M., Gustafsson, Ö., 2014. Sources and light absorption of water-soluble organic carbon aerosols in the outflow from northern China. *Atmos. Chem. Phys.* 14, 1413–1422. <https://doi.org/10.5194/acp-14-1413-2014>.
- LaJeunesse, T.C., Parkinson, J.E., Gabrielson, P.W., Jeong, H.J., Reimer, J.D., Voolstra, C.R., Santos, S.R., 2018. Systematic revision of Symbiodiniaceae highlights the antiquity and diversity of coral endosymbionts. *Curr. Biol.* 28, 2570–2580.e6. <https://doi.org/10.1016/j.cub.2018.07.008>.
- Leinbach, S.E., Speare, K.E., Rossin, A.M., Holstein, D.M., Strader, M.E., 2021. Energetic and reproductive costs of coral recovery in divergent bleaching responses. *Sci. Rep.* 11, 23546. <https://doi.org/10.1038/s41598-021-02807-w>.
- Lesser, M.P., 2013. Using energetic budgets to assess the effects of environmental stress on corals: are we measuring the right things? *Coral Reefs* 32, 25–33. <https://doi.org/10.1007/s00338-012-0993-x>.
- Leuzinger, S., Willis, B.L., Anthony, K.R.N., 2012. Energy allocation in a reef coral under varying resource availability. *Mar. Biol.* 159, 177–186. <https://doi.org/10.1007/s00227-011-1797-1>.
- Levas, S.J., Grotto, A.G., Hughes, A., Osburn, C.L., Matsui, Y., 2013. Physiological and biogeochemical traits of bleaching and recovery in the mounding species of coral *Porites lobata*: implications for resilience in mounding corals. *PLoS One* 8, e63267. <https://doi.org/10.1371/journal.pone.0063267>.
- Li, H., Chen, Y., Zhou, S., Wang, F., Yang, T., Zhu, Y., Ma, Q., 2021a. Change of dominant phytoplankton groups in the eutrophic coastal sea due to atmospheric deposition. *Sci. Total Environ.* 753, 141961. <https://doi.org/10.1016/j.scitotenv.2020.141961>.
- Li, M., Shen, F., Sun, X., 2021b. 2019–2020 Australian bushfire air particulate pollution and impact on the South Pacific Ocean. *Sci. Rep.* 11, 12288. <https://doi.org/10.1038/s41598-021-91547-y>.
- Liu, D., Zhou, C., Keesing, J.K., Serrano, O., Werner, A., Fang, Y., Chen, Y., Masque, P., Kinloch, J., Sadekov, A., Du, Y., 2022. Wildfires enhance phytoplankton production in tropical oceans. *Nat. Commun.* 13, 1348. <https://doi.org/10.1038/s41467-022-29013-0>.
- Luo, Y., Huang, L., Lei, X., Yu, X., Liu, C., Jiang, L., Sun, Y., Cheng, M., Gan, J., Zhang, Y., Zhou, G., Liu, S., Lian, J., Huang, H., 2022. Light availability regulated by particulate organic matter affects coral assemblages on a turbid fringing reef. *Mar. Environ. Res.* 177, 105613. <https://doi.org/10.1016/j.marenvres.2022.105613>.
- Maier, C., Weinbauer, M., Pätzold, J., 2010. Stable isotopes reveal limitations in C and N assimilation in the Caribbean reef corals *Madraca auretenra*, *M. carmabi* and *M. formosa*. *Mar. Ecol. Prog. Ser.* 412, 103–112. <https://doi.org/10.3354/meps08674>.
- Morris, L.A., Voolstra, C.R., Quigley, K.M., Bourne, D.G., Bay, L.K., 2019. Nutrient availability and metabolism affect the stability of coral–Symbiodiniaceae symbioses. *Trends Microbiol.* 27, 678–689. <https://doi.org/10.1016/j.tim.2019.03.004>.
- Muscantine, L., Porter, J.W., Kaplan, I.R., 1989. Resource partitioning by reef corals as determined from stable isotope composition. *Mar. Biol.* 100, 185–193. <https://doi.org/10.1007/BF00391957>.
- Nahon, S., Richoux, N.B., Kolasinski, J., Desmalades, M., Ferrier Pages, C., Lecellier, G., Planes, S., Berteaux Lecellier, V., 2013. Spatial and temporal variations in stable carbon ( $\delta^{13}\text{C}$ ) and nitrogen ( $\delta^{15}\text{N}$ ) isotopic composition of symbiotic scleractinian corals. *PLoS One* 8, e81247. <https://doi.org/10.1371/journal.pone.0081247>.
- Philipp, E., Fabricius, K., 2003. Photophysiological stress in scleractinian corals in response to short-term sedimentation. *J. Exp. Mar. Biol. Ecol.* 287, 57–78. [https://doi.org/10.1016/S0022-0981\(02\)00495-1](https://doi.org/10.1016/S0022-0981(02)00495-1).
- Precht, W.F., 2019. Can *Porites* spp. corals be used as a bio-indicator for sediment stress on coral reefs? *Ecol. Indic.* 106, 105538. <https://doi.org/10.1016/j.ecolind.2019.105538>.
- Price, J.T., McLachlan, R.H., Jury, C.P., Toonen, R.J., Grotto, A.G., 2021. Isotopic approaches to estimating the contribution of heterotrophic sources to Hawaiian corals. *Limnol. Oceanogr.* 66, 2393–2407. <https://doi.org/10.1002/lno.11760>.
- Radice, V.Z., Hoegh-Guldberg, O., Fry, B., Fox, M.D., Dove, S.G., 2019. Upwelling as the major source of nitrogen for shallow and deep reef-building corals across an oceanic atoll system. *Funct. Ecol.* 33, 1120–1134. <https://doi.org/10.1111/1365-2435.13314>.
- Rangel, M., Erler, D., Tagliafico, A., Cowden, K., Scheffers, S., Christidis, L., 2019. Quantifying the transfer of prey  $\delta^{15}\text{N}$  signatures into coral holobiont nitrogen pools. *Mar. Ecol. Prog. Ser.* 610, 33–49. <https://doi.org/10.3354/meps12847>.
- Reichert, J., Arnold, A.L., Hammer, N., Miller, I.B., Rades, M., Schubert, P., Ziegler, M., Wilke, T., 2022. Reef-building corals act as long-term sink for microplastic. *Glob. Chang. Biol.* 28, 33–45. <https://doi.org/10.1111/gcb.15920>.
- Reynaud, S., Martinez, P., Houlbrèque, F., Billy, I., Allemand, D., Ferrier-Pagès, C., 2009. Effect of light and feeding on the nitrogen isotopic composition of a zooxanthellate coral: role of nitrogen recycling. *Mar. Ecol. Prog. Ser.* 392, 103–110. <https://doi.org/10.3354/meps08195>.
- Reynaud-Vaganay, S., Juillet-Leclerc, A., Jaubert, J., Gattuso, J.-P., 2001. Effect of light on skeletal  $\delta^{13}\text{C}$  and  $\delta^{18}\text{O}$ , and interaction with photosynthesis, respiration and calcification in two zooxanthellate scleractinian corals. *Palaeogeogr. Palaeoclimatol. Palaeoecol.* 175, 393–404. [https://doi.org/10.1016/S0031-0182\(01\)00382-0](https://doi.org/10.1016/S0031-0182(01)00382-0).
- Rodrigues, L.J., Grotto, A.G., 2006. Calcification rate and the stable carbon, oxygen, and nitrogen isotopes in the skeleton, host tissue, and zooxanthellae of bleached and recovering Hawaiian corals. *Geochim. Cosmochim. Acta* 70, 2781–2789. <https://doi.org/10.1016/j.gca.2006.02.014>.
- Rogers, C., 1990. Responses of coral reefs and reef organisms to sedimentation. *Mar. Ecol. Prog. Ser.* 62, 185–202. <https://doi.org/10.3354/meps062185>.
- Rosenfeld, M., Bresler, V., Abelson, A., 1999. Sediment as a possible source of food for corals. *Ecol. Lett.* 2, 345–348. <https://doi.org/10.1046/j.1461-0248.1999.00097.x>.
- Ruffault, J., Curt, T., Moron, V., Trigo, R.M., Mouillot, F., Koutsias, N., Pimont, F., Martin-StPaul, N., Barbero, R., Dupuy, J.-L., Russo, A., Belhadj-Khedher, C., 2020. Increased likelihood of heat-induced large wildfires in the Mediterranean Basin. *Sci. Rep.* 10, 13790. <https://doi.org/10.1038/s41598-020-70069-z>.
- Schlösser, J.S., Braun, R.A., Bradley, T., Dadashazar, H., MacDonald, A.B., Aldhaif, A.A., Aghdam, M.A., Mardi, A.H., Xian, P., Sorooshian, A., 2017. Analysis of aerosol composition data for western United States wildfires between 2005 and 2015: dust emissions, chloride depletion, and most enhanced aerosol constituents. *J. Geophys. Res. Atmos.* 122, 8951–8966. <https://doi.org/10.1002/2017JD026547>.
- Schoepf, V., Grotto, A.G., Levas, S.J., Aschaffenburg, M.D., Baumann, J.H., Matsui, Y., Warner, M.E., 2015. Annual coral bleaching and the long-term recovery capacity of coral. *Proc. R. Soc. B Biol. Sci.* 282, 20151887. <https://doi.org/10.1098/rspb.2015.1887>.
- Seemann, J., 2013. The use of  $^{13}\text{C}$  and  $^{15}\text{N}$  isotope labeling techniques to assess heterotrophy of corals. *J. Exp. Mar. Biol. Ecol.* 442, 88–95. <https://doi.org/10.1016/j.jembe.2013.01.004>.
- Siebeck, U.E., Marshall, N.J., Klüter, A., Hoegh-Guldberg, O., 2006. Monitoring coral bleaching using a colour reference card. *Coral Reefs* 25, 453–460. <https://doi.org/10.1007/s00338-006-0123-8>.
- Smith, P.K., Krohn, R.I., Hermanson, G.T., Mallia, A.K., Gartner, F.H., Provenzano, M.D., Fujimoto, E.K., Goeke, N.M., Olson, B.J., Klenk, D.C., 1985. Measurement of protein using bicinchoninic acid. *Anal. Biochem.* 150, 76–85. [https://doi.org/10.1016/0003-2697\(85\)90442-7](https://doi.org/10.1016/0003-2697(85)90442-7).
- Spencer Davies, P., 1989. Short-term growth measurements of corals using an accurate buoyant weighing technique. *Mar. Biol.* 101, 389–395. <https://doi.org/10.1007/BF00428135>.
- Storlazzi, C.D., Norris, B.K., Rosenberger, K.J., 2015. The influence of grain size, grain color, and suspended-sediment concentration on light attenuation: why fine-grained terrestrial sediment is bad for coral reef ecosystems. *Coral Reefs* 34, 967–975. <https://doi.org/10.1007/s00338-015-1268-0>.
- Suggett, D.J., Dong, L.F., Lawson, T., Lawrenz, E., Torres, L., Smith, D.J., 2013. Light availability determines susceptibility of reef building corals to ocean acidification. *Coral Reefs* 32, 327–337. <https://doi.org/10.1007/s00338-012-0996-7>.
- Sundarambal, P., Balasubramanian, R., Tkalic, P., He, J., 2010. Impact of biomass burning on ocean water quality in Southeast Asia through atmospheric deposition: field observations. *Atmos. Chem. Phys.* 10, 11323–11336. <https://doi.org/10.5194/acp-10-11323-2010>.
- Swart, P.K., Szmant, A., Porter, J.W., Dodge, R.E., Tougas, J.I., Southam, J.R., 2005. The isotopic composition of respired carbon dioxide in scleractinian corals: implications for cycling of organic carbon in corals. *Geochim. Cosmochim. Acta* 69, 1495–1509. <https://doi.org/10.1016/j.gca.2004.09.004>.
- Tanaka, Y., Suzuki, A., Sakai, K., 2018. The stoichiometry of coral-dinoflagellate symbiosis: carbon and nitrogen cycles are balanced in the recycling and double translocation system. *ISME J.* 12, 860–868. <https://doi.org/10.1038/s41396-017-0019-3>.
- Tang, W., Lort, J., Weis, J., Perron, M.M.G., Basart, S., Li, Z., Sathyendranath, S., Jackson, T., Sanz Rodriguez, E., Proemse, B.C., Bowie, A.R., Schallenberg, C., Strutton, P.G., Mearns, R., Cassar, N., 2021. Widespread phytoplankton blooms triggered by 2019–2020 Australian wildfires. *Nature* 597, 370–375. <https://doi.org/10.1038/s41586-021-03805-8>.
- Teece, M.A., Estes, B., Gelsleichter, E., Lirman, D., 2011. Heterotrophic and autotrophic assimilation of fatty acids by two scleractinian corals, *Montastraea faveolata* and *Porites astreoides*. *Limnol. Oceanogr.* 56, 1285–1296. <https://doi.org/10.4319/lno.2011.56.4.1285>.
- Thornhill, D.J., Rotjan, R.D., Todd, B.D., Chilcoat, G.C., Iglesias-Prieto, R., Kemp, D.W., LaJeunesse, T.C., Reynolds, J.M., Schmidt, G.W., Shannon, T., Warner, M.E., Fitt, W.K., 2011. A connection between colony biomass and death in Caribbean reef-building corals. *PLoS One* 6, e29535. <https://doi.org/10.1371/journal.pone.0029535>.
- Treyakova, M.O., Vardavas, A.I., Vardavas, C.I., Iatrou, E.I., Stivaktakis, P.D., Burykina, T.I., Mezhuiev, Y.O., Tsatsakis, A.M., Golokhvast, K.S., 2021. Effects of coal microparticles on marine organisms: a review. *Toxicol. Rep.* 8, 1207–1219. <https://doi.org/10.1016/j.toxrep.2021.06.006>.
- Vajed Samiei, J., Saleh, A., Shirvani, A., Sheijooni Fumani, N., Hashtroudi, M., Pratchett, M.S., 2016. Variation in calcification rate of *Acropora downingi* relative to seasonal changes in environmental conditions in the northeastern Persian Gulf. *Coral Reefs* 35, 1371–1382. <https://doi.org/10.1007/s00338-016-1464-6>.
- Wall, C.B., Ritson-Williams, R., Popp, B.N., Gates, R.D., 2019. Spatial variation in the biochemical and isotopic composition of corals during bleaching and recovery. *Limnol. Oceanogr.* 64, 2011–2028. <https://doi.org/10.1002/lno.11166>.
- Wall, C.B., Kaluhiokalani, M., Popp, B.N., Donahue, M.J., Gates, R.D., 2020. Divergent symbiont communities determine the physiology and nutrition of a reef coral across a light-availability gradient. *ISME J.* 14, 945–958. <https://doi.org/10.1038/s41396-019-0570-1>.
- Wang, J.-T., Douglas, A., 1998. Nitrogen recycling or nitrogen conservation in an alga-invertebrate symbiosis? *J. Exp. Biol.* <https://doi.org/10.1242/jeb.201.16.2445>.

- Warner, M.E., Fitt, W.K., Schmidt, G.W., 1999. Damage to photosystem II in symbiotic dinoflagellates: a determinant of coral bleaching. *Proc. Natl. Acad. Sci. USA* 96, 8007–8012. <https://doi.org/10.1073/pnas.96.14.8007>.
- Weber, M., De Beer, D., Lott, C., Polerecky, L., Kohls, K., Abed, R.M.M., Ferdelman, T.G., Fabricius, K.E., 2012. Mechanisms of damage to corals exposed to sedimentation. *Proc. Natl. Acad. Sci. USA* 109. <https://doi.org/10.1073/pnas.1100715109>.
- Weis, V.M., 2008. Cellular mechanisms of cnidarian bleaching: stress causes the collapse of symbiosis. *J. Exp. Biol.* 211, 3059–3066. <https://doi.org/10.1242/jeb.009597>.
- Wiedenmann, J., D'Angelo, C., Smith, E.G., Hunt, A.N., Legiret, F.-E., Postle, A.D., Achterberg, E.P., 2013. Nutrient enrichment can increase the susceptibility of reef corals to bleaching. *Nat. Clim. Chang.* 3, 160–164. <https://doi.org/10.1038/nclimate1661>.
- Xu, R., Yu, P., Abramson, M.J., Johnston, F.H., Samet, J.M., Bell, M.L., Haines, A., Ebi, K. L., Li, S., Guo, Y., 2020a. Wildfires, global climate change, and human health. *N. Engl. J. Med.* <https://doi.org/10.1056/NEJMs2028985>.
- Xu, S., Yu, K., Zhang, Z., Chen, B., Qin, Z., Huang, X., Jiang, W., Wang, Yixuan, Wang, Yinghui, 2020b. Intergeneric differences in trophic status of scleractinian corals from Weizhou Island, northern South China Sea: implication for their different environmental stress tolerance. *Eur. J. Vasc. Endovasc. Surg.* 125 <https://doi.org/10.1029/2019JG005451>.
- Xu, S., Zhang, Z., Yu, K., Huang, X., Chen, H., Qin, Z., Liang, R., 2021. Spatial variations in the trophic status of *Favia palauensis* corals in the South China Sea: insights into their different adaptabilities under contrasting environmental conditions. *Sci. China Earth Sci.* 64, 839–852. <https://doi.org/10.1007/s11430-020-9774-0>.